A GENUINELY MULTIDISCIPLINARY JOURNAL

CHEMPLUSCHEM

CENTERING ON CHEMISTRY

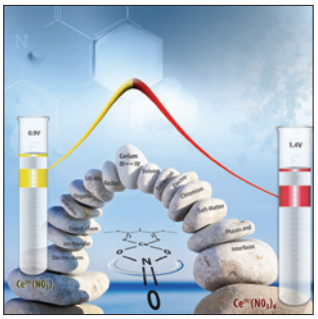

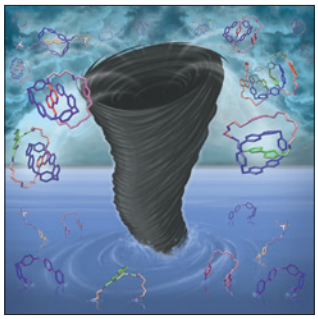

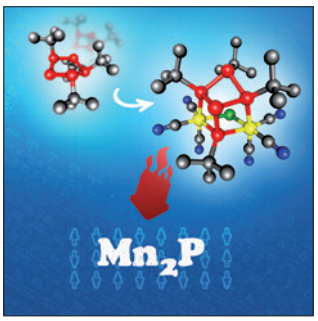

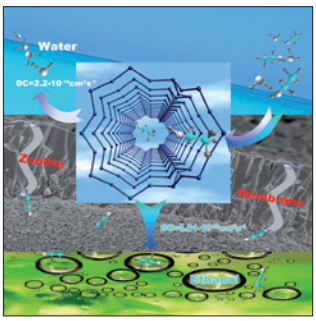

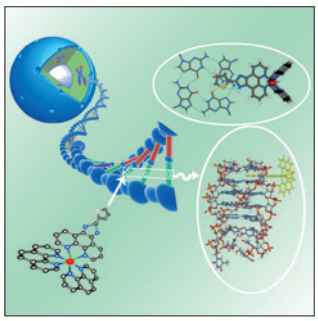


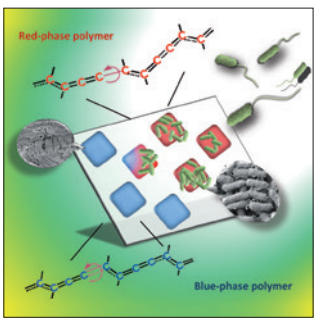

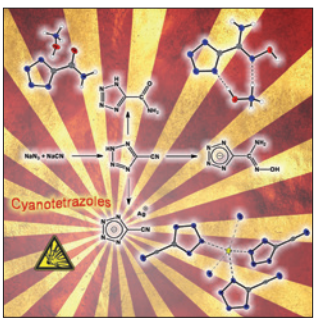

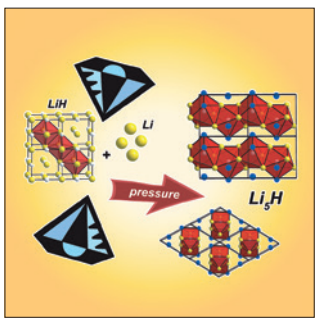

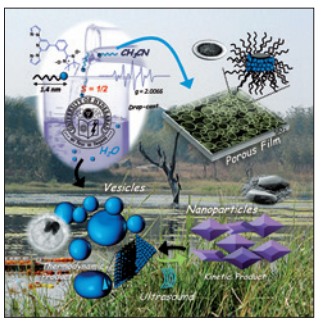

Reprint

A Journal of

ChemPubSoc Europe

WILEY-VCH

www.chempluschem.org

ChemPubSoc Europe

DOI: 10.1002/cplu.201800652

CHEMPLUSCHEM Reviews

SPECIAL ISSUE

Carbonyl-Based π-Conjugated Materials: From Synthesis to Applications in Lithium-Ion Batteries

Hamid Oubaha,[a] Jean-François Gohy,[b] and Sorin Melinte*[a]

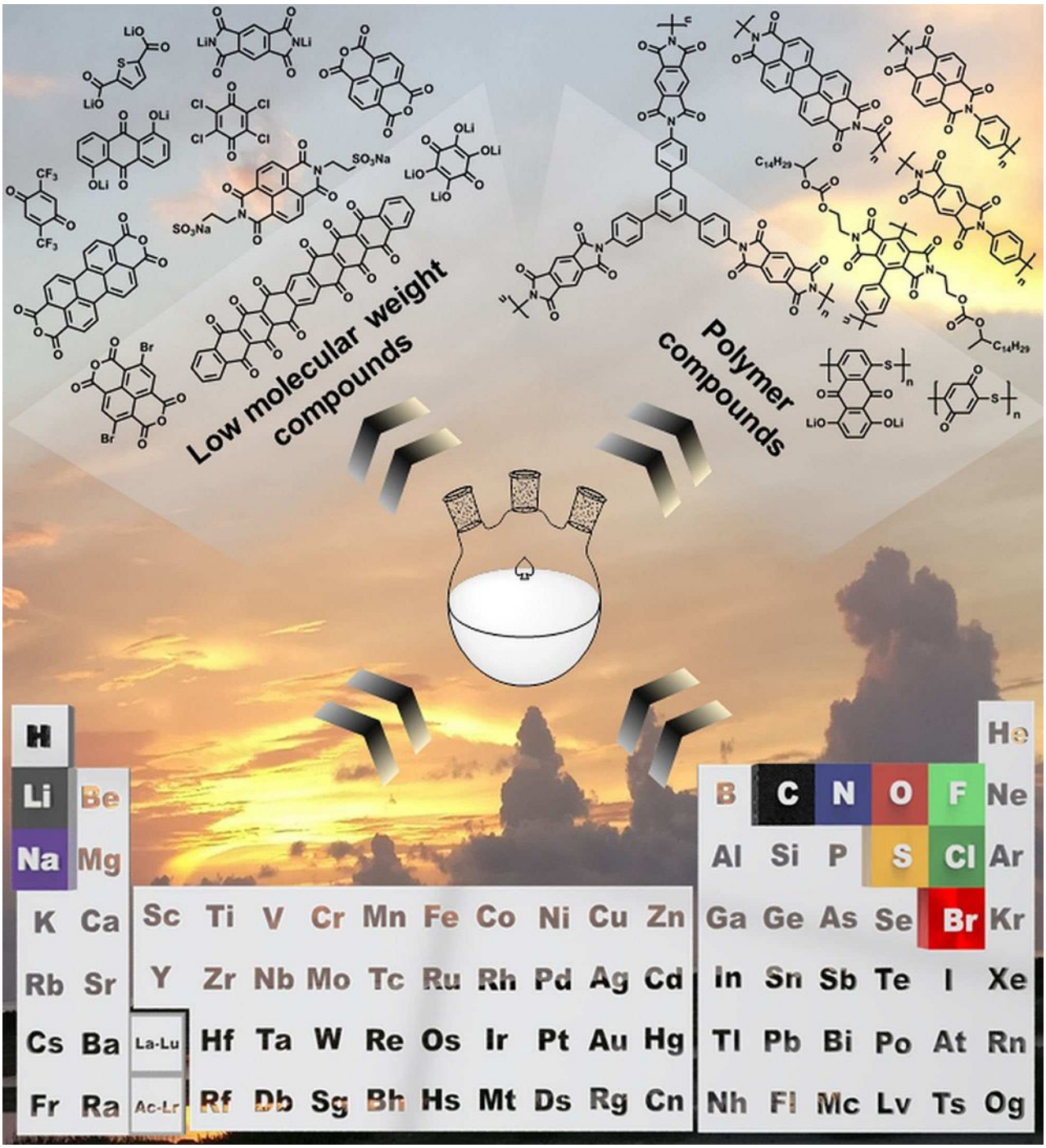

The constant growth in the global energy demand together with the increasing awareness of clean and sustainable development has strongly pushed scientists to search for metal-free, low-cost, environmentally friendly functional energy-storage systems (ESSs). Among the reported organic electrode materials, carbonyl-based π-conjugated compounds show excellent rate capabilities and cycling stabilities and are powerful candidates for the next generation of rechargeable lithium-ion batteries (LIBs). Benefiting from the molecular structure versatility and design feasibility, the electrochemical properties of organic and polymeric materials can be easily tuned. This Review summarizes recent efforts in the search for carbonyl-based π-conjugated electrode materials in LIBs with a focus on the synthetic strategies developed to improve their electrochemical performance. The use of these materials in flexible, all-organic LIBs is highlighted as a unique direction towards widespread applications of LIBs.

Introduction

Energy is literally the lifeblood of our modern societies and continues to be a key element to the worldwide development. However, due to the oil price volatility, depletion of fossil fuel resources, global warming and geopolitical tensions, a transition from fossil fuels to alternative and renewable energies is an urgent global necessity and challenge.[1] For this, the 2015 *U.N. Climate Change Conference* held in Paris, *Conference of the Parties* (COP21), raised the Paris agreement which sets out the worldwide action plan to undertake aspiring efforts to deal with climate change and its impacts. In addition, a real pledge to strengthen the ability of developing countries to follow this direction has been taken.[2] The development of renewable energy sources seems a promising option. Although the availability of renewable energy is plentiful in the form of solar radiation, waves and winds, all are inherently intermittent, generally variable in time and diffuse in space and largely depending on the weather.[3] Hence, in order to make the best use of these energy sources and deliver reliable power to an ever-increasing energy-hungry world caused by the rapid development of electronic devices and electric vehicles, the progress of ESSs represents a major technological challenge for this new century.[1b,4] Among many ESSs, rechargeable batteries are the most promising to meet these requirements of emerging applications.[5]

Rechargeable batteries are devices that store chemical energy with the ability to deliver efficiently this energy as electrical energy with high conversion without gaseous exhaust.[5g,6] In particular, LIBs have been most rapidly developed since *Sony* released the world's first commercial lithium-ion battery in 1991,[5d,6a,7] and their universal impact has been undeniable.

[a] *Dr. H. Oubaha, Prof. S. Melinte*
Institute of Information and Communication Technologies Electronics and Applied Mathematics, Electrical Engineering, Université catholique de Louvain
Place du Levant 3, B-1348, Louvain-la-Neuve (Belgium)
E-mail: sorin.melinte@uclouvain.be
[b] *Prof. J.-F. Gohy*
Institute of Condensed Matter and Nanosciences (IMCN)
Bio- and Soft Matter (BSMA)
Université catholique de Louvain
Place L. Pasteur 1, B-1348, Louvain-la-Neuve (Belgium)

This article is part of a Special Issue on "π-Conjugated (Macro)molecules and their Applications".

The present day market for LIBs is dominated by hard inorganic electrode materials like oxide nanoparticles or nanocoatings like $LiCoO_2$, $LiNiO_2$, $LiMn_2O_4$, $LiFePO_4$, $LiNi_xCo_yMn_{1-x-y}$, for the cathodes[4a,6a] and carbon, Li foils or silicon materials for the anodes.[5f,8] Nonetheless, all these materials have intrinsic limitations in terms of energy-density, which are derived from their redox mechanism of operation and structural aspects.[4f,g,5f] In addition, for some large scale applications as transportation or grid, LIBs based on mineral materials resources are costly at present. Furthermore, they are obtained through high energy consumption processes.[5f,9] The extensive development achieved on various inorganic electrode materials, leads to the theoretical limit of their specific energy.[5f,6a,10] Therefore, safe and environmentally friendly rechargeable batteries with higher energy/power densities are of particular interest at substantially lower cost.[4a,10c,11] As an alternative, research interests begin to change from transition-metal based inorganic materials to organic electrode materials. Owing to the multi-electron reactions, redox stability, structure diversity, processability and flexibility, organic materials consist of low atomic weight and naturally abundant chemical elements (mostly H, C, N, O and S). Moreover, the electronic structure and properties of these materials can be tuned by controlling the synthesis conditions (*i.e.* through the introduction of functional groups), the doping species and doping level.[12] Consequently, organic electrode materials offer new potential for high energy/power density, cycle life, cost-effective, environmentally friendly, functional and safe rechargeable LIBs.[5c,d,12e,13]

While traditional redox reactions in inorganic materials are based on complex intercalation, conversion or alloying mechanisms, organic electrode materials present electro-active features based on reversible electrochemical redox reactions possibly leading to high rate performances and perchance prolonged life.[9d,14] Despite that organic batteries history can be traced back to 1969,[15] much less attention has been paid on organic electrode materials due to the success story of inorganic electrode materials. Fortunately, the research on organic-based batteries evolved in the shadow of the inorganic materials with the discovery of the electronic conductivity of doped conjugated polymers.[12b] Since, many organic electrode materials with various structures have been studied. Based on their electrochemically active functional groups involved in the redox reactions, different types of organic materials have been reported, including conducting polymers (polyacetylene, polyaniline, polypyrrole, polythiophene),[5c,12c,d,16] organo-sulfurs,[17] free radicals (nitroxyl radicals),[8c,18] and carbonyl-based π-

conjugated compounds.[19] The new requirements in energy storage systems such as flexibility and low production costs, specifically for portable, flexible and wearable devices accelerated their development.[5c,14a,20] Particularly, the family of carbonyl compounds is of particular concern to the scientific community thanks to their high reactivity, fast kinetics, high capacity and wide structural design diversity.[4a,5c,21]

The carbonyl group is common to several classes of organic compounds as part of many larger functional groups and displays redox feature. The redox mechanism of carbonyl functionalities implies reversible one-electron reduction to form a radical mono-anion (enolization) and reverse reaction of the carbonyl group (Scheme 1). This can be broadened to more

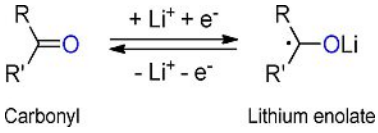

Scheme 1. Typical redox reaction mechanism for an organic cathode material with a carbonyl redox centre.

electrons by an extended conjugated structure.[11a,13a,17] It has been demonstrated that during the electrochemical reaction, lithium ions can be inserted or de-inserted reversibly at oxygen centers when the carbonyl groups are reduced or oxidized.[12e,14b,20c,22]

The research on conjugated carbonyl compounds was initiated by the early work of *Williams et al.* who proposed *di*-chloro-*iso*-cyanuric acid, a positive cathode material with carbonyl functionalities, as a high energy density material for a lithium/*di*-chloro-*iso*-cyanuric acid battery system.[15] Three years later, *Alt et al.* investigated cathode materials based on quinones as reversible redox couples for a rechargeable battery.[21b] These seminal works inspired further synthetic developments and exploitation on carbonyl-based π-conjugated compounds for energy storage technologies. A plethora of studies directed towards the development of carbonyl-based scaffolds is available today.[20c] Typically, carbonyl-based electrode compounds can be classified into four types. Namely, quinones (including polyquinones),[23] imides (including polyimides),[11b,24] anhydrides,[22] and carboxylates (Scheme 2).[12e,19a,20a,c,25]

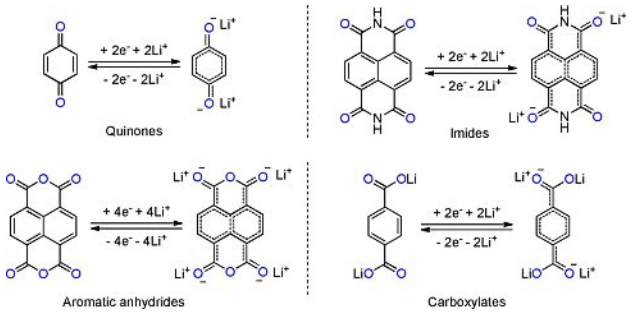

Scheme 2. Schematic representation of the redox reactions of carbonyl-based π-conjugated electrode compounds.

Many excellent reviews with respect to the organic materials containing electroactive carbonyl compounds that contrib-

Hamid Oubaha graduated in Chemical Sciences of Polymer Materials from University of Mons and obtained his PhD in Organic Chemistry and Chemistry of Polymer Materials under the co-supervision of Dr. O. Coulembier and Prof. P. Dubois at the University of Mons and Prof. D. Bonifazi at the University of Namur. He is currently working as a postdoctoral researcher at Institute of Information and Communication Technologies, Electronics and Applied Mathematics, Electrical Engineering (ICTEAM, Université catholique de Louvain, Belgium). His research focuses on the development of novel active materials for Li ions batteries applications.

Sorin Melinte is Professor of Electrical Engineering in the Institute of Information and Communication Technologies, Electronics and Applied Mathematics at Université catholique de Louvain, Belgium. His current projects aim at developing novel nano- and micro-devices and hybrid inorganic-organic platforms for molecular electronics as well as for energy harvesting and storage. In particular, he uses high-resolution electron-beam nanolithography and soft-lithography to link bottom-up and top-down nano- and micro-structuring techniques for the engineering of smart materials.

Jean-François Gohy got his PhD from Prof. Robert Jérôme's group (University of Liège, Belgium) in 1999, working on liquid crystalline ionomers and block copolymers. He then obtained a "Chargé de Recherches" position from the Belgian National Foundation for Scientific Research (FNRS) and started to work on stimuli-responsive block copolymer micelles in the same group. In 2001–2002, he was post-doc in the group of Prof. Ulrich S. Schubert at the Eindhoven University of Technology (The Netherlands) working on metallo-supramolecular polymers. Since 2003, he is Professor at the catholic University of Louvain (Belgium) in the Institute of Condensed Matter and Nanosciences (IMCN). In 2008–2010, he was part-time professor at the Eindhoven University of Technology and invited professor at the University of Bordeaux (France) in 2009. He is author or co-author of more than 210 scientific papers, most of them in the field of functional block copolymers. He has an h-index of 48 (Scopus) and more than 8200 citations.

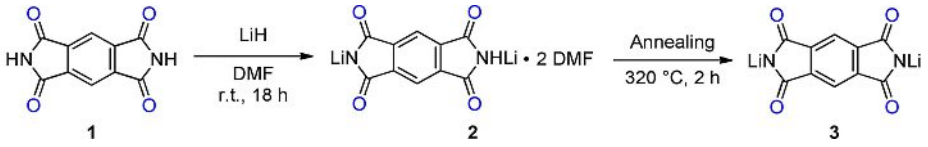

Scheme 3. Synthesis of *di*-lithium pyromellitic *di*-imide salt 3.

ute to LIBs have been reported so far, with a primary focus on the electrode materials.[5c,20b,c,23a] For example, *Schubert* and *co-workers* have summarized the working principle and the structural designs of different carbonyl-based electrode materials for LIBs.[19a] *Xie et al.* classified organic electrodes into three types (anodes, cathodes and bi-functional electrodes) according to their functions along with carbonyl containing π-conjugated electrode materials.[20c] *Tang et al.* discussed recent advancement in carbonyl polymeric electrode materials for lithium-ion, sodium-ion and magnesium-ion batteries.[19c] *Lee et al.* reviewed various strategies for tuning and improving the properties of organic compounds by molecular modification and optimization of their features at the electrode level.[5c]

In the following sections, we aim to give a general, yet concise, overview emphasizing on the organic synthesis and applications of the carbonyl-based π-conjugated electrode materials in the field of LIBs. In particular, through a detailed description of the recent significant examples focusing on the perspectives of molecular synthesis and electrode design, we intend to show that stable carbonyl-based π-conjugated derivatives can be rationally prepared including small molecules and polymers as active electrode materials for high performance organic batteries.

Redox-active Carbonyl-based π-Conjugated Small Molecules for Li–Ion Batteries

Imides Based on π-Conjugated Electrode Active Materials

Low molecular weight aromatic π-conjugated imides, including pyromellitic *di*-imides (**PMDI**),[26] naphthalene *di*-imides[27] (*e.g.* naphthalene-*tetra*-carboxylic *di*-imides (**NTCDI**)), and perylene *di*-imides[28] (*e.g.* perylene-*tetra*-carboxylic *di*-imides (**PTCDI**)) are common n-type semiconductors, and by modulating the π-conjugated backbone linked to the electron-withdrawing carbonyl moieties of the imide, the electron affinity (EA) of the molecule could be tuned, altering thus the LUMO energy levels which guarantee the high redox potential (close to 3 V *vs* Li/Li^+).[11b,19c,28a,29] Interestingly, the carbonyl groups are directly connected to the aromatic core delocalizing the negative charge.[11b,12e] In addition, the redox behaviour of carbonyl compounds can be tuned by the inductive and resonance effects owing to their large structural variety. Despite of being highly soluble in organic electrolytes, small aromatic imide molecules have been successfully applied as active material in organic LIBs.

The first example of the application of small aromatic imide molecules in LIBs reported in the literature is *di*-lithium pyromellitic *di*-imide salt **3**. Described by *Renault et al.*, the active material **3** was prepared by direct lithiation of the commercially available pyromellitic *di*-imide **1** with lithium hydride (LiH) in *N,N-di*-methylformamide (DMF) at room temperature (r.t.) under an inert atmosphere. The high thermal stability of this salt (~570 °C) allowed the elimination of residual DMF molecules by annealing at 320 °C for 2 h affording the final molecule **3** with an overall yield of 91% (Scheme 3).[26] The charge/discharge properties of the battery composed by compound **3** in the presence of 33 wt.% of carbon and 1.0 M lithium bis(trifluoromethanesulfonyl)imide (LiTFSI) in *di*-methyl carbonate (DMC) electrolyte revealed a two-stage redox behaviour with plateaus at 1.81 and 1.62 V corresponding to the two one-electron redox reactions. Moreover, 93% of material activity with the uptake of 1.86 Li per formula unit (220 $mAh \cdot g^{-1}$) and the removal of 1.66 Li on the subsequent charge were observed, leading to practical reversible capacities above 200 $mAh \cdot g^{-1}$ on dozens of cycles.

The presence of different substituents in the carbonyl based conjugated molecules can affect not only the chemical structure of the active material but also the electrochemical properties. For instance, *Coskun* and *co-workers* investigated the effect of the substitution on the *N*-positions on the electrochemical performance of LIBs based on naphthalene *tetra*-carboxylic *di*-imides (**NDIs**).[27c] Thus, three different **NDI** derivatives, in which the imide nitrogens are functionalized with -H (*1,4,5,8*-naphthalene *tetra*-carboxylic *di*-imide, **NDIH**) **5**, -Li (*di*-lithium naphthalene *di*-imide salt, **NDILi**) **6** and $-CH_3$ (*N,N'-di*-methyl-*1,4,5,8*-naphthalene *tetra*-carboxylic *di*-imide, **NDIMe**) **7** groups were synthesized according to the reported methods in the literature. Therefore, *1,4,5,8*-naphthalene *tetra*-carboxylic *di*-anhydride (**NTCDA**) **4** reacts in a concentrated aqueous solution of ammonium hydroxide (NH_4OH) at r.t. affording **NDIH 5** in 96% yield.[30] When **NDIH 5** was reacted with LiH in DMF at r.t. followed by annealing at 200 °C, the *di*-lithium salt **NDILi 6** was obtained in 96% yield. The presence of aqueous $MeNH_2$ and $PhNO_2$ gave **NDIMe 7**[31] (Scheme 4). As indicated by the electrochemical analyses, **NDIH 5** exhibits a broad charge/discharge plateau between 2.41 and 2.64 V, accompanied by only 40% capacity retention after 100 cycles at 0.5 C (compared to its initial capacity of 170 $mAh \cdot g^{-1}$). While, the introduction of methyl groups (**NDIMe**, **7**) at both nitrogen centers prohibits tautomerism, it increases the dissolution of the molecule in the electrolyte, leading to severe capacity decay and leads to a rapid decrease of the materials' activity upon cycling. In contrast, superior electrochemical performance was obtained by lithiation of both nitrogen atoms (**NDILi**, **6**). Due to a lower

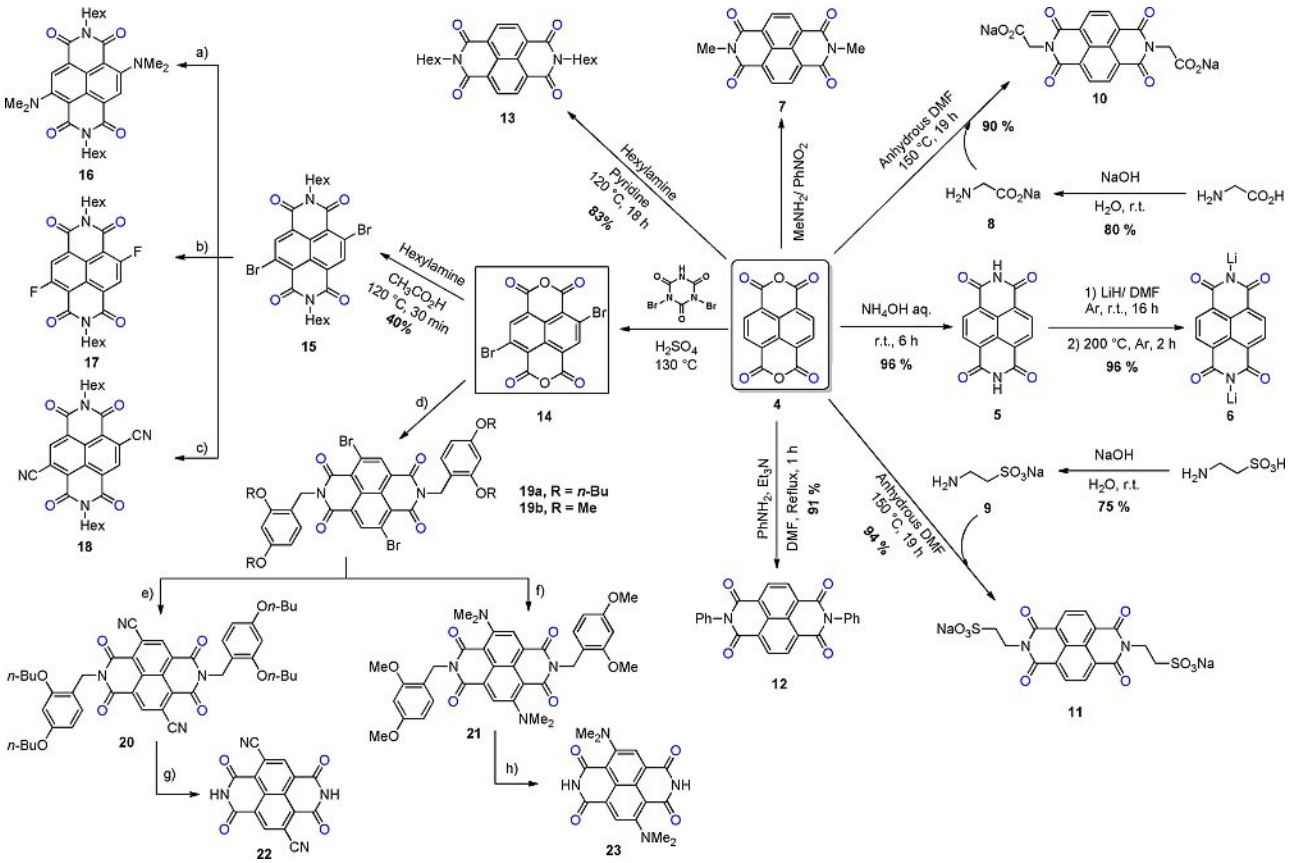

Scheme 4. Synthetic pathways of substituted NDI derivatives. Reagents and conditions: a) *Di*-methyl-amine, THF, 80 °C, 12 h, 93 %. b) KF, *18*-crown-*6*, 3 Å molecular sieves, sulfolane, 165 °C, 45 min, 53 %. c) CuCN, NMP, 100 °C, 2 h, 87 %. d) *Di*-alkoxybenzyl amine, acetic acid 120 °C. e) CuCN, NMP 100 °C, 3 h, 70 %. f) *Di*-methylamine, THF, 95 °C, 20 h, 13 %. g) (*i*) $MeSO_3H$, PhMe, 110 °C, 4 h; (*ii*) $SOCl_2$, DMF, r.t., 90 min, 81 %. h) $MeSO_3H$, PhMe, 110 °C, 4 h, 79 %.

solubility in the electrolyte and the aromatization in its lithiated state, **NDILi** displayed 89 % capacity retention (117 $mAh \cdot g^{-1}$ after 100 cycles at 0.5 C) and a broader charge/discharge plateau (2.65 to 2.0 V).[27c]

Similarly to the previously discussed study, and to circumvent the unwanted solubility in usual organic electrolytes of the small molecular weight active materials, *Lakraychi et al.* reported the *N*-substitution on naphthalene *tetra*-carboxylic *di*-imide (**NDIs**) ionic compounds having a carbon chain spacer between the nitrogen atom and the anionic groups, namely, methyl-sodium carboxylate (**NTCDI(MeCarb-Na)$_2$**) **10** and ethyl-sodium sulfonate (**NTCDI(EtSulf-Na)$_2$**) **11** salts.[32] The two molecules were synthesized by reaction of naphthalene *tetra*-carboxylic *di*-anhydride **4** with neutralized glycine and taurine, in 90 % and 94 % yields, respectively (Scheme 4). The electrochemical behaviors of the two active materials mixed with carbon black (30 wt.%) have been investigated in a carbonate-based liquid electrolyte. Both compounds showed an important decrease of solubility in the carbonate-based liquid electrolyte, in conjunction with a very stable cycle performances with a very good capacity retention of 147 $mAh \cdot g^{-1}$ for **10** and 113 $mAh \cdot g^{-1}$ for **11** as well as high coulombic efficiency (CE) ~99 % over 50 cycles.

In the report by *Chou* and *co-workers* in 2016, *N,N′-di*-phenyl-*1,4,5,8*-naphthalene *tetra*-carboxylic *di*-imide (**DP-NTCDI-250**) **12** was synthesized as new cathode active material for LIBs.[33] The synthesis was performed through a one-pot *N*-acylation reaction of *1,4,5,8*-naphthalene *tetra*-carboxylic *di*-anhydride **4** using aniline in the presence of *tri*-ethylamine (Et_3N) in DMF under refluxing, the desired compound **DP-NTCDI-250 12** was prepared in 91 % yield (Scheme 4). **DP-NTCDI-250 12** showed an initial discharge capacity of 170 $mAh \cdot g^{-1}$ at the current density of 25 $mAh \cdot g^{-1}$ with a retaining capacity of 119 $mAh \cdot g^{-1}$ after 100 cycles. The capacity remained at 105 $mAh \cdot g^{-1}$ even at the high current density of 500 $mAh \cdot g^{-1}$, indicating its high rate capability.

Aiming to increase the voltage of **NDIs** in lithium-ion batteries, *Dunn* and *co-workers* introduced substituents with different electronic effects onto the **NDI** core. Compounds with electron donating groups –NMe_2 (**16** and **23**) and electron withdrawing –F (**17**) and –CN (**18** and **22**) were considered.[27b] The synthetic routes to prepare different **NDI** derivatives are described in Scheme 4. When molecule **4** is reacted with hexylamine in pyridine at 120 °C, compound **13** could be obtained in 83 % yield. While the reaction of the molecule **4** with *di*-bromo-*iso*-cyanuric acid in the presence of H_2SO_4 at 130 °C gave access to the highly functionalized *4,9-di*-bromo-*iso*-chromeno[*6,5,4-def*]*iso*chromene-*1,3,6,8-tetra*-one **14** as molecular precursor for preparing a suitable naphthalene *di*-imides bearing different substituents. In particular, the reaction

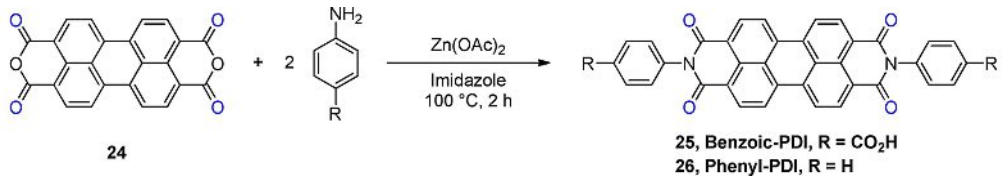

Scheme 5. Synthesis of benzoic-PDI 25 and phenyl-PDI 26.

between the derivative **14** with hexylamine in acetic acid at 120 °C afforded the intermediate **NDI 15** in 40%. While the treatment of the molecule **15** with *di*-methyl-amine in *tetra*-hydro-furan (THF) at 80 °C led to the product **16** in 93% yield, the use of KF and *18*-crown-*6* in *tetra*-methylene sulfolane at 165 °C gave the desired fluorinated derivative **17** in 53% yield and copper(I) cyanide (CuCN) in *N*-methyl pyrrolidone (NMP) at 100 °C afforded the cyano-derivative **18** in 87% yield. In other hand, removable protecting groups (alkoxybenzyl) were used to confer solubility during the synthesis and purification of all intermediates. Thus, the reaction of the compound **14** with *di*-alkoxybenzyl amine in acetic acid at 120 °C gave access to alkoxybenzyl-**NDI** derivatives **19a** and **19b**. The reaction of compound **19a** with CuCN in NMP led to the molecule **20** which was converted to the cyano-**NDI** derivative **22** by methanesulfonic acid and thionyl chloride in toluene. In parallel, **NMe_2-NDI 23** was obtained in 79% yield by the deprotection in toluene of *di*-methoxybenzyl groups of compound **19b** using methanesulfonic acid. The attachment of cyano groups to the **NDI** core in compound **22** increases the voltage from 2.55 V in the parent compound **5** to 2.90 V *vs* Li/Li^+ for the first reduction. When the *di*-imide nitrogens were functionalized with hexyl groups (compounds **16**, **17** and **18**), the capacity faded rapidly due to dissolution in the organic electrolyte.[27b] However, when the *N*-unsubstituted compounds are used (compounds **22** and **23**), a higher cycling stability is observed but with a low capacity due to an unfavourable crystal packing. The electronic effects brought by the substituents influence the electrochemical properties of the NDI-based compounds resulting in electrodes with discharge potentials that vary from 2.3 to 2.9 V *vs* Li/Li^+, with discharge capacities as high as 121 $mAh \cdot g^{-1}$.

Besides the naphthalene tetra-carboxylic *di*-imide derivatives, *3,4,9,10*-perylene *tetra*-carboxylic *di*-imide derivatives (**PDIs**) have been probed as electrode active materials for LIBs. Recently, *Bhosale et al.* found chemically reduced redox active carboxylic acid and phenyl containing *3,4,9,10*-perylene *tetra*-carboxylic *di*-imide molecules (**benzoic-PDI**) **25** and (**phenyl-PDI**) **26** with hydrazine that can increase the rate of redox reaction as well as the conductivity and consequently improve the electrochemical performance in LIB applications.[28a] The **25** and **26** compounds were synthesized by reacting *3,4,9,10*-perylene *tetra*-carboxylic *di*-anhydride (**PTCDA**) **24** with *4*-aminobenzoic acid and aniline, respectively, in the presence of zinc acetate and imidazole at 100 °C for 2 h (Scheme 5). The reduction of **benzoic-PDI 25** or **phenyl-PDI 26** with hydrazine leads to an improvement in the electrochemical performances of the electrodes fabricated in presence of carbon black (30 wt.%) as conductive material and *Kynar* (10 wt.%) as a binder. The specific capacity for reduced **benzoic-PDI 25** was reported to be 85 and 107 $mAh \cdot g^{-1}$ at 1 C and 10 C, respectively, compared to the 60 and 30 $mAh \cdot g^{-1}$ at 1 C and 10 C for the untreated **benzoic-PDI 25**. Moreover, **benzoic-PDI 26** cathode exhibits 100% CE, increased specific capacity when discharging at 20 C and very good stability.

In a parallel study, a series of commercially available, perylene *di*-imide derivatives bearing different substituents at *N*-centers (H-, methyl, *4*-methoxy-phenyl, *4*-ethoxy-phenyl, *3,5-di*-methyl-phenyl, Scheme 6) were examined by *Zhu et al.* as

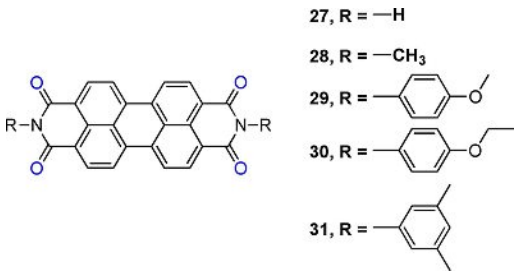

Scheme 6. Molecular structures of commercially available *N*-substituted perylene *di*-imide derivatives structures tested as electrode materials.[28b]

cathode active materials for Li-storage system.[28b] The Li-ion batteries consisted of perylene *di*-imide powders, conductive carbon, poly(*tetra*-fluoro-ethylene) (PTFE) binder (60/30/10 wt.%) and Li metal as counter electrode. For the electrolyte, 1.0 M $LiPF_6$ solution in ethylene carbonate (EC)/*di*-ethyl carbonate (DEC)/propylene carbonate (PC) (4/5/1 v/v/v) was used. Despite the introduction of different substituent at *N*-position, similar charge/discharge behaviours as **PTCDI 27** were obtained for the different substituted perylene *di*-imides with a redox capacities up to 130 $mAh \cdot g^{-1}$, good rate capability and cycling stability at flat discharge potential plateau around 2.4 V.

In the 2016 report by *Wasielewski* and *co-workers*, the synthesis of G-quadruplex organic framework **G_2PDI 38** composed of *n*-hexyl-substituted perylene *di*-imide *N*-functionalized with two guanine derivatives as an organic cathode material for Li-ion battery has been described (Scheme 7).[34] The synthesis of **G_2PDI 38** was started by fully Boc-protection of N^9-octyl-*8*-bromo-guanine **32** in the presence of *4-di*-methylaminopyridine (DMAP), *di-tert*-butyl *di*-carbonate (Boc_2O) and *di-iso*-propyle-thylamine $(i\text{-}Pr)_2EtN$) in DMF at 30 °C for 48 h leading to N^9-

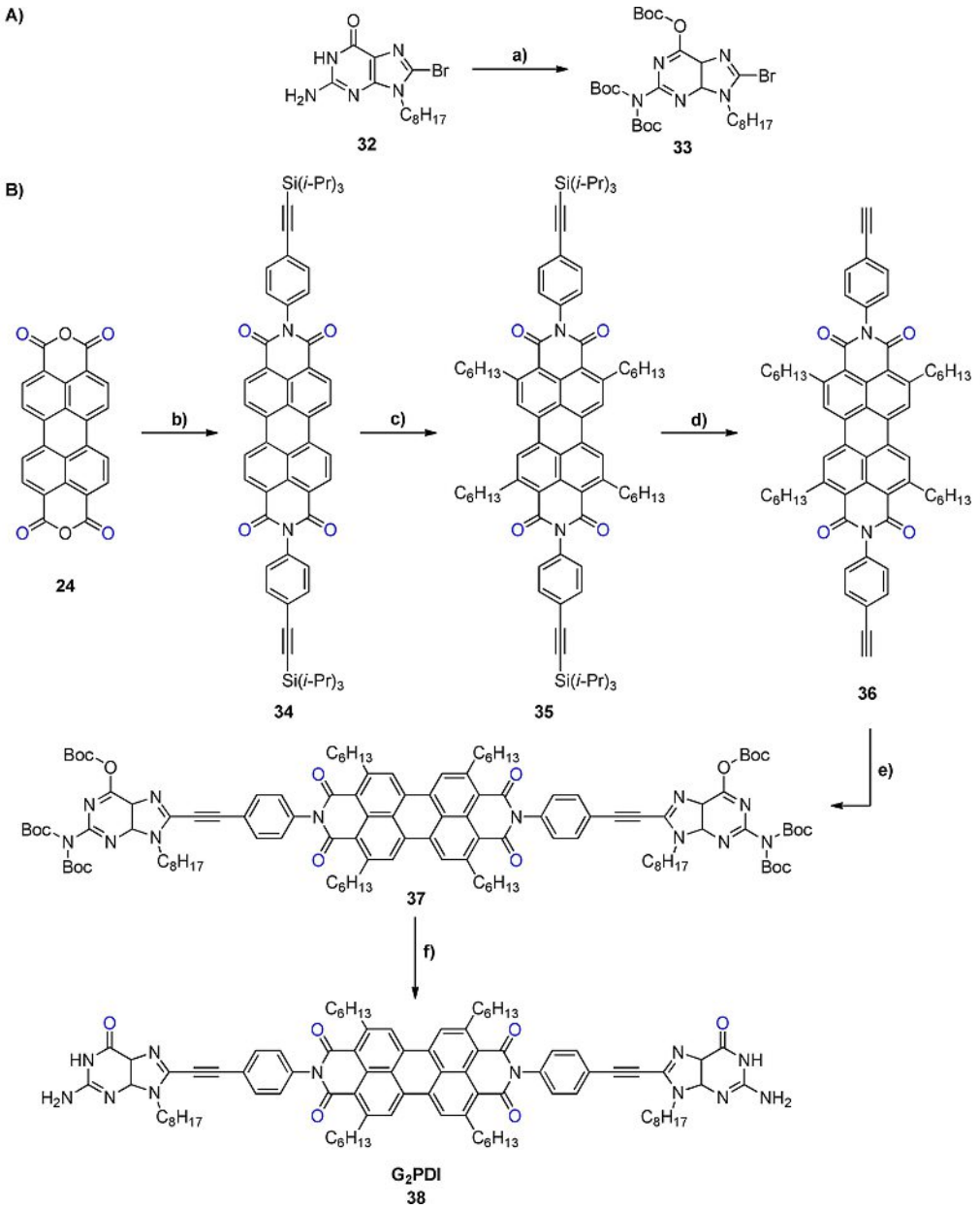

Scheme 7. Preparation of G_2PDI 38. Reagents and conditions: a) DMAP, Boc_2O, *i*-Pr_2EtN, DMF, 30 °C, 48 h, 74%. b) *4*-((*tri-iso*-propylsilyl)ethynyl)aniline, Zn $(OAc)_2 \cdot 2H_2O$, quinoline, 150 °C, 16 h, 79%. c) $[Ru(PPh_3)_3(CO)H_2]$, *1*-hexene, mesitylene, N_2 atmosphere, 195 °C, 5 d, 72%. d) *n*-Bu_4NF, THF, 2% H_2O, r.t., 15 h, 91%. e) Boc_3GBr 33, $[Pd(PPh_3)_3]$, CuI, Et_3N, THF, N_2-atmosphere, 50 °C, 40 h, 43%. f) *i*) CF_3CO_2H, CH_2Cl_2, 40 h, *ii*) CH_3OH, 24 h, *iii*) DMF, 50 °C, 5 d, quant. $[Ru(PPh_3)_3(CO)H_2]$: carbonyl *di*-hydrido-*tris*(*tri*-phenylphosphine)ruthenium(II), $[Pd(PPh_3)_3]$: *tetrakis*(*tri*-phenylphosphine)palladium(0).

octyl-*8*-bromo-guanine (**Boc_3GBr**) **33** in 74% yield (Scheme 7, reaction a). In parallel, *4*-[(*tri-iso*-propylsilyl)ethynyl]aniline was used to functionalize the perylene-*3,4,9,10-tetra*-carboxylic *di*-anhydride **24** using $Zn(OAc)_2 \cdot 2H_2O$ in quinolone at 150 °C leading to *N,N-bis*{*4*-[(*tri-iso*-propylsilyl)ethynyl] phenyl} perylene-*3,4:9,10*-bis(*di*-carboximide) **34** in 79% yield (Scheme 7, reaction b). Then the solubility of the PDI intermediates was improved by selective introduction of *n*-hexyl chains at the 2, 5, 8 and 11 positions using $[Ru(PPh_3)_3(CO)H_2]$, *1*-hexene, mesitylene under N_2-atmosphere at 195 °C (Scheme 7, reaction c). Silyl groups were then removed by *n*-Bu_4NF in THF containing 2% H_2O at r.t. providing the *bis*-ethynylated PDI **36** in 91% yield (Scheme 7, reaction d). Finally, the compound **G_2PDI 38** was prepared via *Sonogashira* cross coupling reaction between *bis*-acetylene PDI derivative **37** and the Boc-protected guanine **Boc_3GBr 33** using $[Pd(PPh_3)_3]$, CuI and Et_3N in THF under N_2-atmosphere at 50 °C followed by fully removing of the Boc-groups with *tri*-fluoroacetic acid (TFA) in CH_2Cl_2 (Scheme 7, reaction e and f). The G-quadruplex organic framework was obtained by vapour exchange between CH_2Cl_2/TFA and CH_3OH and soaking in DMF at 50 °C for 5 days. The porous structure and the electrons transport capability of **G_2PDI 38**, while maintaining its structural stability, has pushed the authors to test this compound as cathode materials in a Li-ion battery. The

composite electrode was fabricated by mixing compound **G_2PDI 38**, conductive carbon black and poly(vinylidene fluoride) (PVdF) binder (80/10/10 wt.%). For tests, Li metal was used as counter electrode and 1.0 M solution of $LiPF_6$ in EC/DMC (1/1 v/v) as electrolyte. Galvanostatic charge/discharge cycling analysis at 10 $mA \cdot g^{-1}$ of the **G_2PDI 38** based LIB showed two plateaus around 1.8 and 2.3 V in agreement with the cyclic voltammogram which exhibited two reversible peaks around 1.9 and 2.3 V corresponding to the two redox stages of **G_2PDI 38**. An initial capacity of 27 $mAh \cdot g^{-1}$, with a good capacity retention and coulombic efficiency after 300 cycles, was attributed to the framework structure stability.

Anhydride Based π-Conjugated Active Materials

Able to undergo up to two-electron reductions favoring reversible insertion of lithium ions at the oxygen atoms of the anhydride functional group, aromatic anhydrides can be used as active compounds in ESSs (Scheme 2).[22] Described by *Ohzuku et al.* in 1979, the commercially available pyromellitic *di*-anhydride (**PMDA**) **39** (Scheme 8) was the first anhydride-containing material applied in LIBs.[35] It had a theoretical capacity of 246 $mAh \cdot g^{-1}$ based on two-electron transfer with an open circuit voltage of 3.1–3.2 V. The specific capacity of **PMDA 39** cathode was doubled (~500 $mAh \cdot g^{-1}$) by the addition of 18 wt.% of pyromellitic acid (**PA**) **40** as proton donor in the presence of 40 wt.%, of acetylene black and 1.0 M $LiClO_4$ in PC as electrolyte.

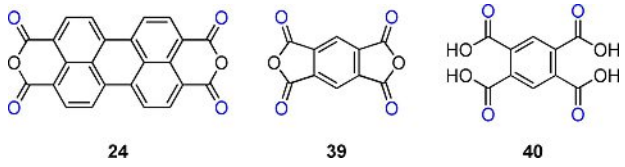

Scheme 8. Chemical structure of aromatic anhydrides (*3,4,9,10*-perylene *tetra*-carboxylic *di*-anhydride (PTCDA) 24, pyromellitic *di*-anhydride (PMDA) 39 and pyromellitic acid (PA) 40 applied as cathode active materials in LIBs.

Further, *Sun et al.* reported *3,4,9,10*-perylene *tetra*-carboxylic acid *di*-anhydride **24** (Scheme 8), which had an initial capacity of 135 $mAh \cdot g^{-1}$ showing however, a poor cycling stability (60% loss over 80 cycles) due to the dissolution in the electrolyte.[22] In a different work, the authors studied the reversible intercalation of lithium ions into an aromatic anhydride system containing *1,4,5,8*-naphthalene *tetra*-carboxylic *di*-anhydride **4** (Scheme 4).[36] The electrochemical study unfolded five distinct discharge plateaus corresponding to the insertion of 1, 2, 4, 8, and 18 Li ions at discharge potentials of 2.340, 1.690, 1.040, 0.470, and 0.001 V. Despite the 18 Li-ions per *1,4,5,8*-naphthalene-*tetra*-carboxylic *di*-anhydride molecule could be inserted by reduction of the carbon-carbon double bonds at low potential (superlithiation mechanism),[36b] only four lithium ions can be reversibly inserted through a lithium enolization reaction at the four carbonyl oxygen atoms.

In 2017, large aromatic *di*-anhydride structures based on naphthalene and perylene scaffolds, naphthalene *tetra*-carboxylic *di*-anhydride (**NDA-4N**, **44**) and perylene *tetra*-carboxylic acid *di*-anhydride (**PDA-4N**, **48**), containing four nitrogen atoms were investigated by *Xie et al.* as organic cathode materials for LIBs (Scheme 9).[37] The synthesis of **NDA-4N 44** and **PDA-4N 48** was achieved following the same conditions for both building blocks. First, *di*-anhydride molecule (**4** or **34**) was refluxed overnight with DBU, *2*-ethyl-*1*-hexanol and *2*-ethylhexyl bromide in CH_3CN affording compounds **41** (93% yield) or **45** (73% yield) (Scheme 9, reaction a). The treatment of molecule

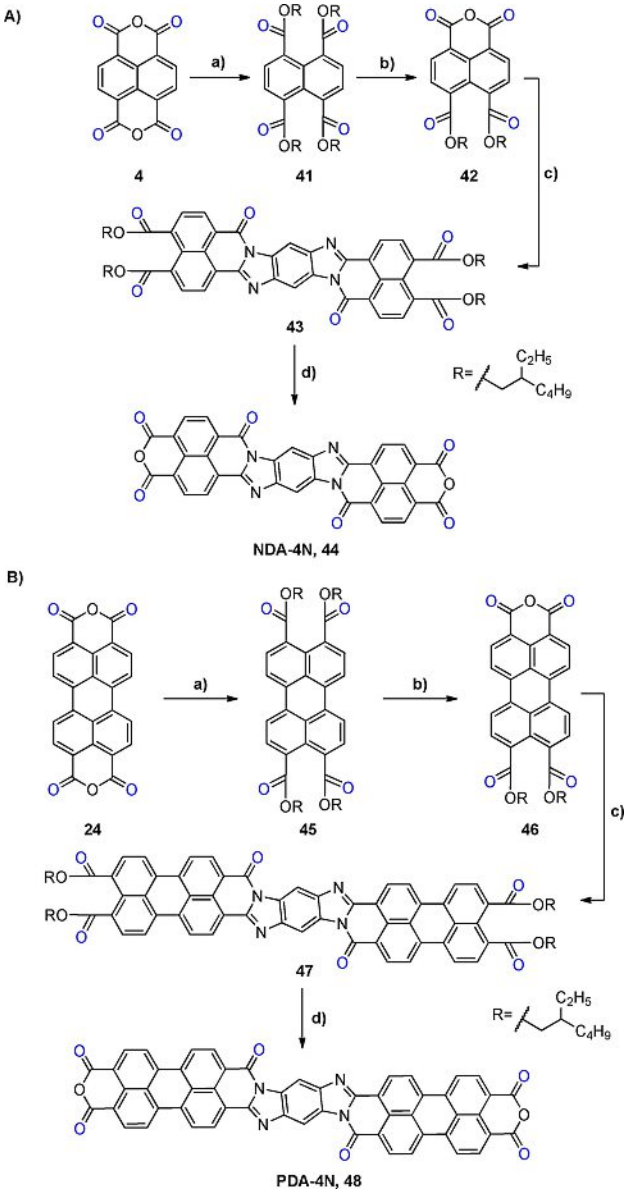

Scheme 9. Synthetic pathways of A) NDA-4N 44 and B) PDA-4N 48. Reagents and conditions: a) DBU, *2*-ethyl-*1*-hexanol, *2*-ethylhexyl bromide, CH_3CN, reflux, overnight 41 (93%), 45 (73%). b) *p*-Toluene sulfonic acid monohydrate ($TsOH \cdot H_2O$), toluene, heptane, 110 °C, 24 h, 42 (37%), 46 (95%). c) Pyridine, *1,2,4,5-tetra*-aminobenzene *tetra*-hydrochloride, Ar-atmosphere, reflux, overnight, 43 (58%), 47 (41%). d) $TsOH \cdot H_2O$, toluene, 110 °C, 24 h, NDA-4N 44 (96%), PDA-4N 48 (95%). DBU: *1,8-di*-aza-*bi*-cyclo[*5.4.0*]undec-*7*-ene, $TsOH \cdot H_2O$: *p*-toluene sulfonic acid monohydrate.

41 or **45** with *p*-toluene sulfonic acid monohydrate ($TsOH \cdot H_2O$) in toluene/heptane mixture at 110 °C for 24 h led to the mono-anhydride derivative **42** (37% yield) or **46** (95% yield) (Scheme 9, reaction b). The mono-anhydride molecules **42** and **46** were reacted with *1,2,4,5-tetra*-aminobenzene *tetra*-hydrochloride in pyridine under Ar-atmosphere overnight affording compounds **44** and **47** in 58% and 41% yields, respectively. Finally, *di*-anhydrides **NDA-4N 44** and **PDA-4N 48** were obtained in 96% and 95% yields, respectively, by the treatment of compounds **44** and **47** with $TsOH \cdot H_2O$ in toluene at 110 °C for 24 h. The tested electrodes were consisting of the active materials (**NDA-4N 44** or **PDA-4N 48**), carbon nanotubes (CNTs) and PVdF (30/50/20 wt.%). For tests, Li metal was used as the counter electrode and 1.0 M solution of LiTFSI in *di*-methoxyethane (DME)/*1,3-di*-oxolane (DOL) (1/1 v/v) containing 1% $LiNO_3$ as the electrolyte. Initial reversible capacities of 141.8 $mAh \cdot g^{-1}$ and 116.4 $mAh \cdot g^{-1}$ were observed for **NDA-4N 44** and **PDA-4N 48**, respectively. The specific capacity of **NDA-4N 44** faded during cycling to 48.8 $mAh \cdot g^{-1}$ after 99 cycles at a current density of 66 $mA \cdot g^{-1}$, while **PDA-4N 48** retained 70.9% of the initial capacity after 99 cycles at the same current density. The authors demonstrated a 36.5% of improvement of the capacity by enlarging the structure from the naphthalene to the perylene building block.

Quinones Based π-Conjugated Active Materials

Low molecular weight quinones represent the most widely studied molecules for Li-ions battery cathodes due to their two-electron reduction reactions that provide a high theoretical capacity with fast and reversible electrochemical reactions.[12i,23a] The first quinoide structure used as active material in a Li-organic battery was *di*-chloro-*iso*-cyanuric acid **49** (Scheme 10)[15] and the redox mechanism of the quinoide

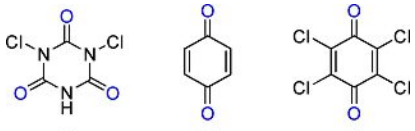

49 **50** **51**

Scheme 10. Chemical structure of *di*-chloro-*iso*-cynauric acid 49, benzoquinone (BQ) 50 and *2,3,5,6-tetra*-chlorocyclohexa-*2,5*-diene-*1,4-di*-one (chloranil) (TCB) 51.

system was first reported in 1972.[21b] Benzoquinone (**BQ**) **50** (Scheme 10) as the most simple quinone compound, presents a high specific capacity (496 $mAh \cdot g^{-1}$).[12i,38] Unfortunately, serious volatility and solubility issues prevent direct use of **BQ** in conventional LIBs.[39] Nevertheless, the introduction of electron withdrawing groups like chlorine, nitrile and fluorine or rigid groups such as *2,3,5,6-tetra*-phthalimide into the benzoquinone framework should yield an organic active material electrode with high specific capacity and stable cycling performance. Thus, *Alt et al.* studied the application *tetra*-chlorine-substituted benzoquinone namely *2,3,5,6-tetra*-chlorocyclohexa-*2,5*-diene-*1,4-di*-one (chloranil) **TCB 51** (Scheme 10) as an electrode active material for batteries using aqueous acid or organic electrolyte.[21b] Due to the stabilizing capability of chlorine substituents, the battery could be charged/discharged over 50 cycles (~95% material activity at 0.5 C) with a negligible capacity loss, in the presence of 5 M sulfuric acid as electrolyte and a graphite rod as the counter electrode.

Recently, another effort to improve the cycling stability and working potential of LIBs cathodes was achieved by *Zhao* and *co-workers*. Two benzoquinones namely *2,3-di*-chloro-*5,6-di*-cyano-*1,4*-benzoquinone (**DDQ**) **52** and *2,3-di*-chloro-*5*-hydroxy-*6*-cyano-*1,4*-benzoquinone (**DHCQ**) **53** were investigated and compared as organic electrode materials.[40] **DHCQ 53** was synthesized in 80% yield through a simple chemical hydrolysis of **DDQ 52** at r.t. (Scheme 11). Lithium-ion batteries manufac-

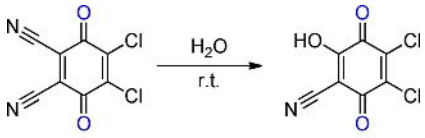

52 **53**

Scheme 11. 2,*3-di*-chloro-*5*-hydroxy-*6*-cyano-*1,4*-benzoquinone (DHCQ) 53.

tured from composite electrodes containing **DDQ 52** or **DHCQ 53**, carbon black, PTFE binder and 1.0 M $LiPF_6$ in ethyl carbonate (EC) and DMC electrolyte displayed an initial discharge capacity up to 2000 $mAh \cdot g^{-1}$ at a specific current of 50 $mA \cdot g^{-1}$. A reversible charge capacity of 1009 $mAh \cdot g^{-1}$ was retained after 50 cycles with a high coulombic efficiency (CE) above 98%, higher than that of **DDQ 52** under the same rate (579 $mAh \cdot g^{-1}$ after 50 cycles) with a long term cycling stability (capacity retention of about 78% after 400 cycles at 500 $mA \cdot g^{-1}$). The authors attributed the high reversible capacities to the surface adsorption of lithium ions.[40–41] However, the reversible lithium insertion on the unsaturated bonds could lead to the 'super-lithiation' process.

Another approach to increase the voltage of quinone-based cathodes is the introduction of electron withdrawing groups onto the quinone-based chemical structures. Interestingly, *Yokoji* and *co-workers* evaluated benzoquinones bearing perfluoroalkyl groups as positive electrode materials in rechargeable LIBs.[42] Fluorinated benzoquinones **58a** (**CF_3-BQ**), **58b** (**RF_9-BQ**) and **58c** (**RF_{13}-BQ**) were synthesized following the procedures outlined in Scheme 12. The treatment of *1,4-di*-methoxybenzene **54** with I_2 and HIO_3 afforded *2,5-di*-iodo-*1,4-di*-methoxybenzene **55** in 76% yield. The *di*-iodide compound **55** was then converted to perfluoroalkyl compounds **56a–c** using copper-catalyzed perfluoroalkylation. The reaction of molecule **55** with CF_3CO_2Na and Cu(I)I afforded *1,4-di*-methoxy-*2,5-bis*(*tri*-fluoromethyl)benzene **56a** in 52% yield, while reacting **55** with perfluorobutyl iodide C_4F_9I or $C_6F_{13}I$ in the presence of CuI and *2,2'*-bipyridine gave access to *1,4-di*-methoxy-*2,5*-bis(perfluoro-butyl)benzene **56b** and *1,4*-dimethoxy-*2,5*- bis(perfluorohexyl)

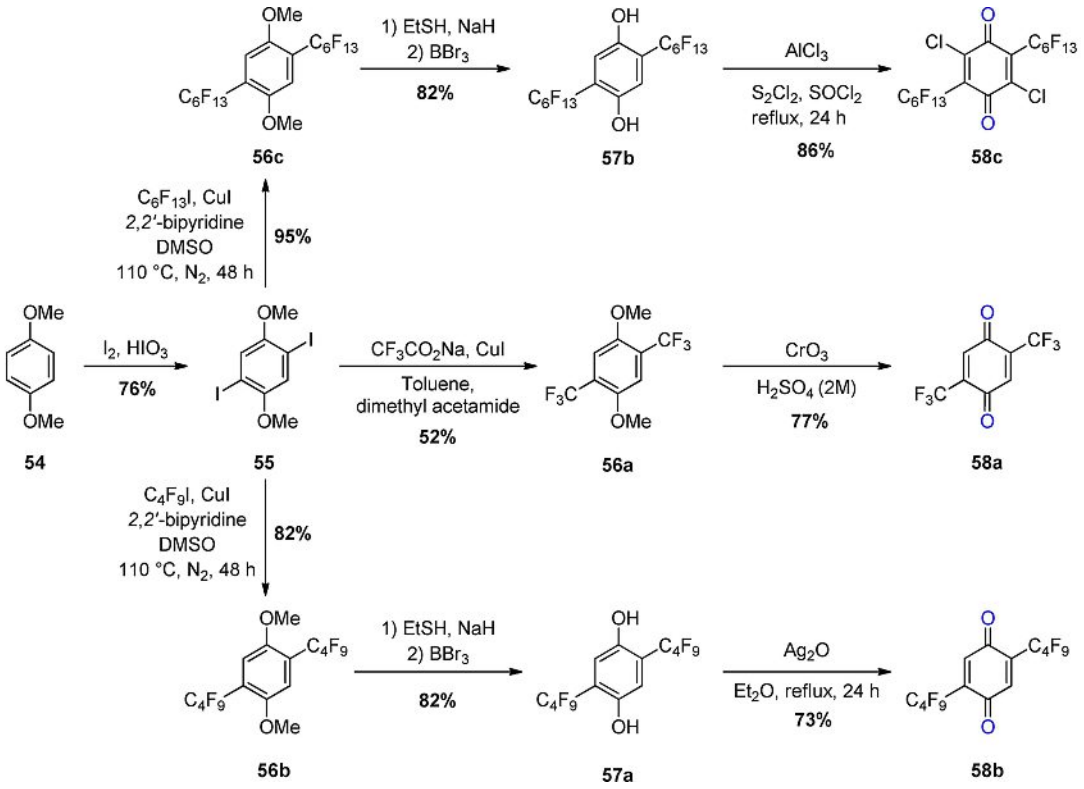

Scheme 12. Synthetic pathways of fluorinated benzoquinones CF_3-BQ 58a, RF_9-BQ 58b and RF_9-BQ 58c.

benzene **56c** in 82% and 95% yield, respectively. *Di*-methoxy groups removal was achieved using sodium ethanethiolate (EtSNa) and BBr_3 affording hydroquinone derivatives **57a** and **57b** which were oxidized to benzoquinones **58b** (**RF_9-BQ**) using Ag_2O/Et_2O and **58c** (**RF_{13}-BQ**) using $S_2Cl_2/SOCl_2$ in the presence of $AlCl_3$ in 73% and 86% yields, respectively. The use of CrO_3 and H_2SO_4 allowed demethylation and oxidation of the compound **56a** affording the CF_3-substituted benzoquinone **58a** (**CF_3-BQ**) in 77% yield.[43] Lithium organic batteries manufactured with these **BQ**s were examined using 1.0 M $LiPF_6$ in EC/DEC (3/7 v/v) as electrolyte, vapor-grown carbon fiber (VGCF) as the conductive material and PTFE as the binder. When compared to *2,5-bis*-(methyl)cyclohexa-*2,5*-diene-*1,4-di*-one (**CH_3-BQ**), fluorinated electron-withdrawing groups improve the voltage by up to 600 mV from 2.5 V for **CH_3-BQ** to 3.1 V *vs* Li/Li^+ for **58b** and **58c**, with improved charge-discharge cycle performance in the cells due to a stabilization of the radical and *di*-lithiated intermediate by lithium-fluorine interactions and the stability of the benzoquinones toward decomposition during cycling. However, a strong decrease in capacities over cycling was observed.

In a similar approach, *Luo et al.* reported *2,3,5,6-tetra*-phthalimido-*1,4*-benzoquinone (**TPB**) **59** as an organic electrode in which the benzoquinone skeleton is rigidly coordinated by four phthalimide moieties.[44] The synthesis of **TPB 59** was performed by the treatment of chloranil (**TCB**) **51** with potassium phthalimide in refluxed CH_3CN under N_2 atmosphere for 12 h affording the desired compound **TPB 59** (Scheme 13). Through the introduction of rigid groups, **TPB 59** addresses the

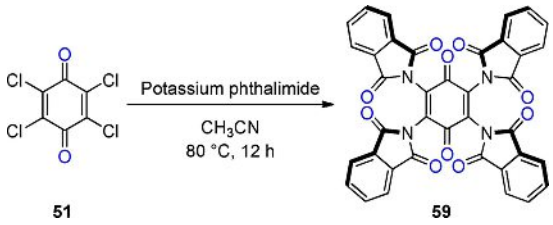

Scheme 13. Synthesis of *2,3,5,6-tetra*-phthalimido-*1,4*-benzoquinone TPB 59.

challenge of high solubility of organic electrodes in aprotic electrolytes. Compared to **TCB 51** a high capacity retention of 91.4% (204 $mAh \cdot g^{-1}$) over 100 cycles at 0.2 C was achieved (Figure 1). Besides, density functional theory investigations demonstrated an enhancement of the initial lithium ion intercalation potential due to concerted reactions between multiple oxygen centers and lithium ions.[45] Although increasing the size of the aromatic structure decreases the solubility in usual organic electrolytes and can yield large theoretical capacities, upon reduction, electrostatic repulsions could be imposed by the sterically hindered and close redox groups limiting the specific capacity. In addition, this may mix up the crystal packing resulting in dissolution in the liquid electrolyte and capacity fading.

Increasing the molecular size of the quinone-based active material could also settle the solubility issues and increase the stability during the lithiation. For that purpose, *Boschi et al.* have proposed a larger polycyclic derivative, nonylbenzohexaquinone **NBHQ 62**.[46] Presenting a poor solubility in organic

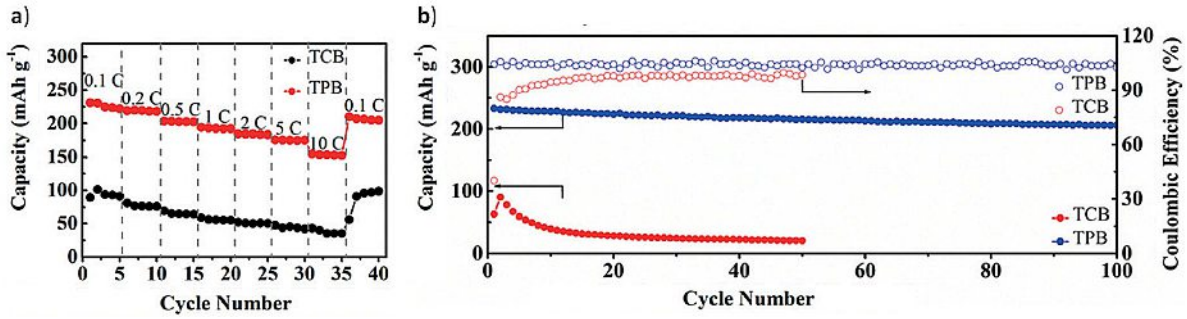

Figure 1. a) Rate performance and b) long-term cycling performance of TPB 59 and TCB 51 at 0.2 C. Reproduced with permission.[44] Copyright 2017, Wiley-VCH Verlag GmbH & Co. KGaA, Weinheim.

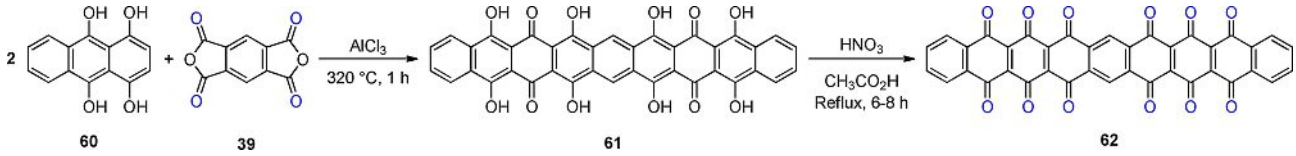

Scheme 14. Synthesis of nonylbenzohexaquinone NBHQ 62.

solvents and a high theoretical capacity (489 $mAh \cdot g^{-1}$) (if all 12 electrons are involved in the charge storage process), **NBHQ 62** has been used as positive electrode active material for LIBs.[46] Reinvestigated further by *Pasquali et al.*,[47] **NBHQ 62** was basically prepared by a double condensation of leucoquinizarin (anthracene-*1,4,9,10-tetra*-ol) **60** and pyromellitic *di*-anhydride **39** in the presence of $AlCl_3$ at 320 °C for 1 h. The resulting *octa*-hydroxy-*di*-quinone **61** was then oxidized to **NBHQ 62** using fuming HNO_3 in refluxing glacial CH_3CO_2H (Scheme 14). A lithium organic battery using 1.0 M $LiClO_4$ in PC/DME (1/1 v/v) mixture as electrolyte and Li metal as counter electrode was tested. A cell voltage of 3.0 V and a capacity of 125 $mAh \cdot g^{-1}$ (26% of material activity) could be achieved at a charging speed of C/2, which faded to 115 $mAh \cdot g^{-1}$ after 500 charge/discharge cycles. The average energy density during this cycling was 160 $Wh \cdot kg^{-1}$.

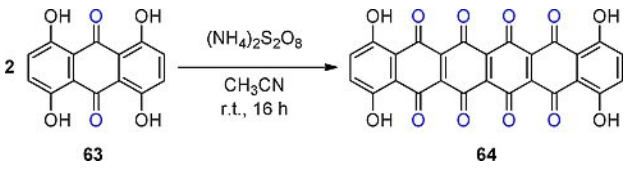

Scheme 15. Synthesis of *tetra*-hydro-*hexa*-quinone 64.

Aiming to both decrease the solubility and increase the capacity of quinones, *Zou et al.* synthesized the *tetra*-hydro-*hexa*-quinone **64** from the commercially available *1,4,5,8-tetra*-hydroxy-*9,10*-anthracene-*di*-one **63** using $(NH_4)_2S_2O_8$ in CH_3CN at r.t. (Scheme 15).[48] At the current density of 200 $mA \cdot g^{-1}$, the initial specific capacity was 340 $mAh \cdot g^{-1}$ which is about 54.1% of the theoretical capacity (~628 $mAh \cdot g^{-1}$). A specific capacity of 203 $mAh \cdot g^{-1}$ was retained after 40 cycles. However, when the current density was increased to 800 $mA \cdot g^{-1}$, the capacity dropped to 26.5%.

To tune the voltage and to decrease the solubility in organic electrolytes of carbonyl containing molecules without adding EWGs or rigid groups, the usance of organic metal salts represents a promising solution, especially organic Li salts. In this respect, *Poizot* and *co-workers* studied the *tetra*-lithium salt of *tetra*-hydroxy-benzoquinone (*tetra*-lithioxy-benzoquinone) **67** as the active material in Li-organic batteries.[49] The synthesis of the *tetra*-lithioxy-benzoquinone **67** could be achieved through two synthetic pathways; *i*) the solid-state disproportionation reaction at 400 °C under argon atmosphere of *di*-lithium rhodizonate **65** and *ii*) the deprotonation at r.t. of *tetra*-hydroxy-benzoquinone **66** using a CH_3OLi solution in anhydrous CH_3OH (Scheme 16). Lithium-organic batteries of the designed molecule **67** exhibited an initial capacity of ~200 $mAh \cdot g^{-1}$ (77% active material) with only a capacity decay of 10% after 50

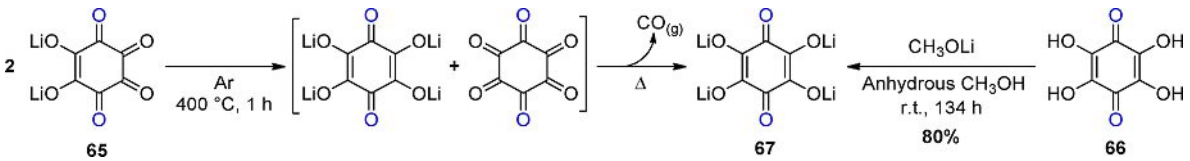

Scheme 16. Synthesis of *tetra*-lithiooxybenzoquinone 67 by *i*) solid-state disproportionation reaction of *di*-lithium rhodizonate 65 under argon flow and *ii*) the deprotonation of *tetra*-hydroxybenzoquinone 66.

cycles at a rate of 1 C for an average cell voltage of 1.8 V. Interestingly, improved electrochemical performances were observed with the compound obtained by the solid-state disproportionation reaction, due probably to the production of extra carbon during the process.

In a follow-up study, the same group examined the electrochemical performance of the lithiated *3,6*-dihydroxy-*2,5*-dimethoxy-*p*-benzoquinone (**Li_2DHDMQ**) **70**.[50] The three-step synthetic route to synthesize the compound **Li_2DHDMQ 70** was started with the preparation of *tetra*-methoxy-*p*-benzoquinone (**TMQ**) **68**. This consists of the reaction of chloranil **51** with a solution of sodium methanolate CH_3ONa. The lithium salt was obtained by a simple saponification procedure in which **TMQ 68** was treated with LiOH in water. Lyophilization of the trihydrate form **Li_2DHDMQ·3H_2O 69** followed by annealing at 180 °C under vacuum for 2 h afforded the crystallized **70** (Scheme 17). A lithium-organic battery equipped with the active

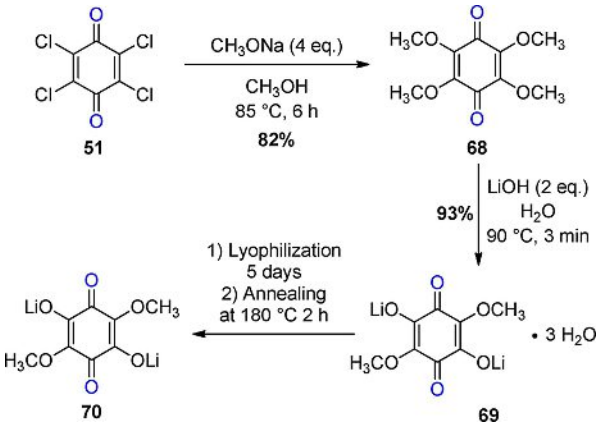

Scheme 17. Synthesis of *3,6-di*-hydroxy-*2,5-di*-methoxy-*p*-benzoquinone (Li_2DHDMQ) 70. PLEASE CHECK POSITION ON PAPER BEFORE SCHEME 18!

material **Li_2DHDMQ 70** and 33 wt.% carbon SP using Li metal as negative electrode and 1.0 M $LiPF_6$ solution in EC/DMC (1/1 v/v) as electrolyte showed two-stage charge/discharge behaviour at 3.1 V involving one-electron in the oxidation and at 2.2 V corresponding to the two-electron reduction. The battery exhibited an initial capacity of 136 mAh·g^{-1} (54% material activity) which dropped to 12% material activity (30 mAh·g^{-1}) after 50 cycles at 0.16 C. The addition of 10 wt.% γ-Al_2O_3 nanoparticles to the composite electrode allowed the maintain of the capacity at 32% material activity (80 mAh·g^{-1}) after 50 cycles.

When a polymer electrolyte like LiTFSI/poly(ethylene oxide) (PEO)[51] or solid electrolyte (*e.g.* LISICON, $Li_{2+2x}Zn_{1-x}GeO_4$)[52] is applied in the battery, there is a great opportunity for small organic molecules to be used because of the elimination of the dissolution problem. In this view, the group of *Poizot* investigated the use of **TMQ 68** (Scheme 17) as redox-active molecule for its expected two-electron reaction which leads to an expected specific capacity of 235 mAh·g^{-1}, using the commercially available LiTFSI/PEO-based solid polymer electrolyte (O/Li molar ratio = 25) at 100 °C.[53] A reversible capacity of about 80% of the theoretical value (190 mAh·g^{-1}) could be delivered after 20 cycles at a rate of 1 Li/30 min with remarkable power performance. Besides, the diffusion of **TMQ 68** through the electrolyte film could not be fully prevented as attested by the colour of the electrolyte, which, had turned to the typical orange colour of **TMQ 68** without apparent degradation.

Zeng et al. used the lithium salt of *1,5-di*-hydroxyanthraquinone, $Li_2(C_{14}H_6O_4)$ **73**, as a lithium-inserted material for LIBs.[54] The synthesis of the targeted molecule **73** was achieved by dehydration reaction at 300 °C under N_2 atmosphere of [$Li_2(C_{14}H_6O_4)$·H_2O] complex **72** obtained through the reaction of deprotonation of the *1,5-di*-hydroxyanthraquinone **71** with LiOH in ethanol under N_2 atmosphere at 80 °C for 48 h (Scheme 18). The lithium-organic battery equipped with composite materials of compound **73**, 15 wt.% acetylene black, 5 wt.% PTFE binder and 1.0 M $LiPF_6$ in ethyl methyl carbonate (EMC)/EC/DMC (1/1/1 v/v/v) electrolyte exhibited an initial capacity of 115 mAh·g^{-1} at an average potential of 1.8 V and current density of 111 mA·g^{-1}. The discharge capacity remains at 100 mAh·g^{-1} (47% material activity) after 50 charge/discharge cycles at a speed of 0.5 C. Acting as electron donating groups, lithio-oxy groups lead to a shift of the redox potential to lower values, thus, becoming a severe drawback for the use of this salt as cathode active material.

To circumvent this issue, an alternative approach consisting in the introduction of two lithium carboxylate groups into the *p*- and *o*-quinone structures was developed. For instance, *Wang et al.* investigated the *tetra*-lithium salt of *2,5-di*-hydroxyterephthalic acid $Li_4C_8H_2O_6$ (**Li_4DHTPA**) **76** as the active material of either positive or negative electrode of rechargeable LIBs.[14b] The *tetra*-lithium salt **76** was synthesized by the reaction of *2,5-di*-hydroxyterephthalic acid (**DHTPA**) **74** with lithium methoxide (CH_3OLi) followed by annealing the complex **75** at 220 °C (Scheme 19, reaction a). Electrodes composed of compound **76**, carbon black and PVdF binder with 1.0 M $LiPF_6$ in EC/DMC (1/1 v/v) electrolyte, demonstrated reversible two-electron electrochemical reactions occurring with redox couples of $Li_4C_8H_2O_6$/$Li_2C_8H_2O_6$ in the positive electrode. The nanosheet morphology showed the best electrochemical performance with an initial discharge capacity of 223 mAh·g^{-1} and a capacity retention

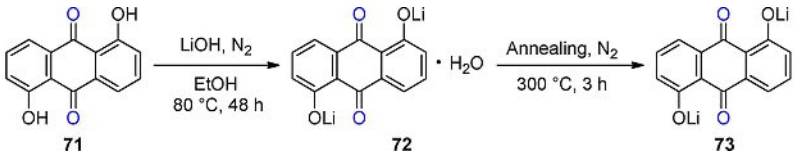

Scheme 18. Synthesis of $Li_2(C_{14}H_6O_4)$ 73.

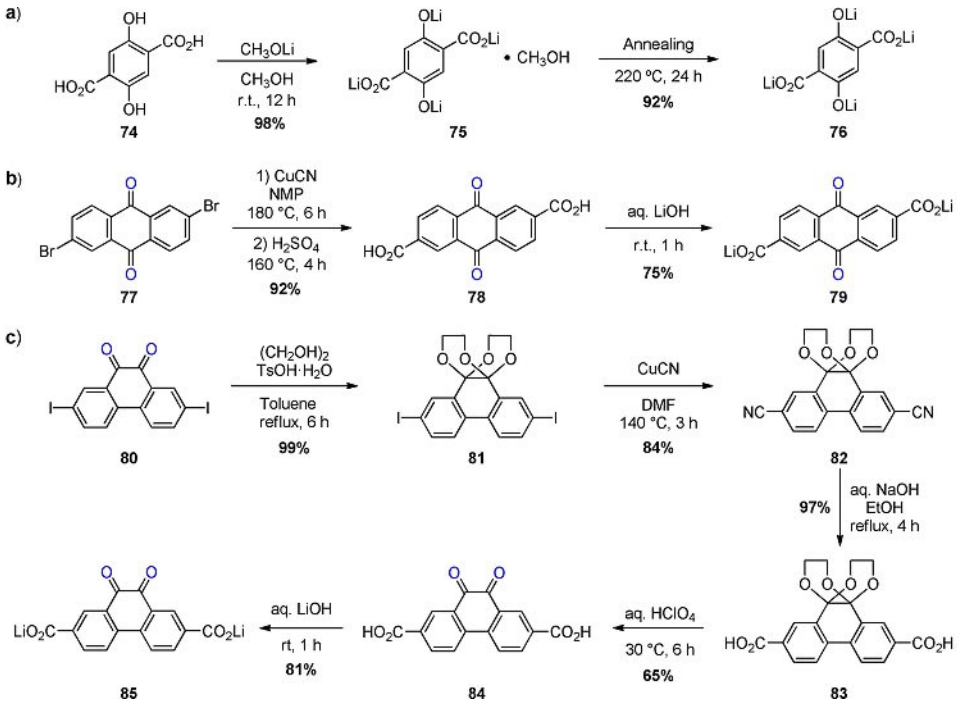

Scheme 19. Synthesis of a) Li_4DHTPA 76, b) LCAQ 79 and c) LCPQ 85.

exceeding 95% after 50 cycles at 0.1 C rate with a CE close to 99.9%.

Yoshida and *co-workers* studied the effect of lithiocarboxy groups on the cycling stability of the *2,6-bis*-(lithiooxycarbonyl)-*9,10*-anthraquinone (**LCAQ**) **79** and *2,7-bis*-(lithiooxycarbonyl)-*9,10*-phenanthrenequinone (**LCPQ**) **85**.[55] The **LCAQ 79** was synthesized from *2,6-di*-bromo-*9,10*-anthraquinone **77**. Cyanation of compound **77** and subsequent acidic hydrolysis of the cyano groups gave the *di*-carboxylic acid **78** which was neutralized by LiOH to give the **LCAQ 79** in 75% yield (Scheme 19, reaction b). On the other hand, **LCPQ 85** was synthesized from *2,7-di*-iodo-*9,10*-phenanthrenequinone **80**. Protection of the *o*-quinone structure of **80** with *1,2*-ethanediol gave the protected *di*-iodo-compound **81** in a quantitative yield. Cyanation of **81** with CuCN and subsequent hydrolysis of the cyano groups gave the protected *di*-carboxylic acid **83**. Deprotection of **83** gave the compound **84** in 65% yield, which was neutralized with LiOH leading to the targeted molecule **LCPQ 85** in 81% yield (Scheme 19, reaction c). When compared to the compounds without lithiocarboxy groups, both molecules showed an improvement in the cycling stability attributed to strong intermolecular interactions between the lithiooxycarbonyl groups preventing dissolution. Moreover, the tested batteries were composed of active material **79** or **85**, acetylene black, PTFE (1.5, 4.0, 1.0 wt.%) and electrolyte 1.0 M $LiPF_6$ in PC. The two electrodes exhibited a stable capacity, but poor energy storage properties. Only capacities of 85 $mAh \cdot g^{-1}$ (49% active material) and 90 $mAh \cdot g^{-1}$ (50% material activity) were obtained over 20 cycles at a charge/discharge speed of 0.2 C for **79** and **85**, respectively. In addition, no significantly change was noticed in the voltage.

Park and *co-workers* synthesized naphthoquinone derivatives *2,3-di*-amino-*1,4*-naphthoquinone (**DANQ**) **88** and *1*H-naphtho[*2,3-d*]imidazole-*4,9*-dione (**IMNQ**) **89** as cathode materials for LIBs.[56] The compound **DANQ 88** was prepared in 90% yield following *Gabriel* reaction using potassium phthalimide and hydrazine hydrate. Refluxing formic acid with **DANQ 88** for 5 h afforded the desired molecule **IMNQ 89** in 83% yield (Scheme 20). Cathodes were consisting in **DANQ 88** (or **IMNQ 89**), carbon Super P (SP), and PVdF binder (60/30/10 wt.%). Li metal was used as the counter electrode and 1.0 M LiTFSI in DME/DOL (1/2 v/v) as electrolyte. On the one hand, **DANQ 88** displayed an initial discharge capacity of 250 $mAh \cdot g^{-1}$ with a 99% capacity retention after 500 cycles (248 $mAh \cdot g^{-1}$) and high coulombic efficiency of up to 99% at 0.2 C rate. On the other

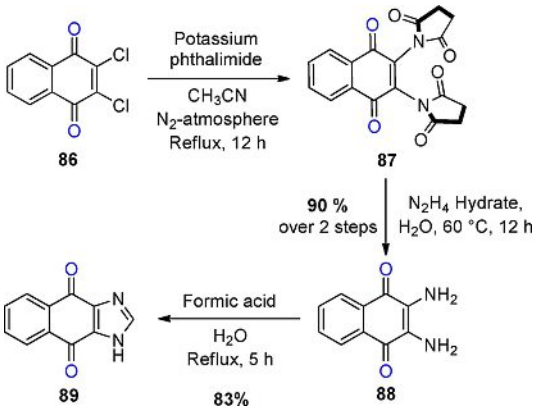

Scheme 20. Synthetic approaches toward the preparation of DANQ 88 and IMNQ 89.

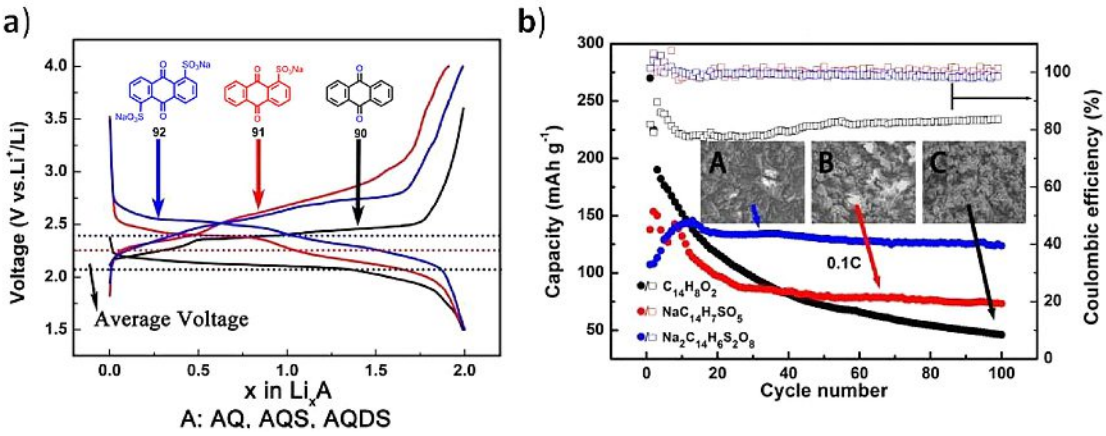

Figure 2. a) Charge and discharge curves and b) cycle performance and CE of AQ 90, AQS 91, and AQDS 92 electrodes cycled at 0.1 C rate. The SEM images of the three compounds are shown in the inset pictures. Reproduced with permission.[57] Copyright 2014, Royal Society of Chemistry.

hand, the **IMNQ 89** showed 240 mAh·g^{-1} initial capacity which declines to 152 mAh·g^{-1} after 100 cycles at 0.2 C rate.

Another strategy to improve the cycling stability and also raise the reduction potential of the quinone derivatives is the functionalization of quinone moieties with ionic groups to prevent dissolution in organic electrolytes. In this respect, *Wan et al.* investigated the anthraquinone (**AQ**) **90** which was functionalized to form *mono*- and *di*-sodiumsulfate anthraquinones (**AQS**) **91** and (**AQDS**) **92**.[57] When studied in LIBs, both compounds exhibit high specific capacities, 130 and 150 mAh·g^{-1} at 0.2 C for **AQ 90** and **AQS 91**, respectively. The additional ionic group improves not only the solubility issue and the thermal stability (525 °C for **AQDS 92** *vs* 257 °C for **AQ 90** under N_2), but the cycling performance was enhanced from 50 % to 92 % after 100 cycles at 0.1 C with a raise of the average reduction potential by 150 mV due to the extra electron-withdrawing effect. Interestingly, no obvious capacity fading can be observed during cycling and reversible specific capacity of 120 mAh·g^{-1} can be retained after 100 cycles for **AQDS 92** (Figure 2).

π-Conjugated Carboxylic Acids as the Active Materials for Lithium-Ion Batteries

The low redox potential of n-type organic π-conjugated compounds (*e.g.*, 0–1.5 V *vs* Li/Li$^+$) allowed applying them as anode active material in LIBs.[12h,17] For their part, π-conjugated carboxylates are able to undergo a reversible two-electron redox reaction. In addition, coupled with low polarization, less strain and low solubility in the electrolyte they have gained great attention as alternative anode materials for LIBs. The redox center of π-conjugated carboxylates is located in the weakly electron-withdrawing carboxyl groups, and the redox process involves the resonance of π-conjugated bonds in the carbon chain or aromatic core whereby the resulting *di*-anion is stabilized by a conjugated system.[12e]

Similar to cathodes, the strategies applied on organic anodes also aims to increase the capacity and the cycling stability. For instance, in 2009, *Tarascon* and *co-workers* reported for the first time that π-conjugated carboxylates can be utilized as the active electrode material for LIBs.[12e] The *di*-lithium terephthalate ($Li_2C_8H_4O_4$) **94** and *di*-lithium muconate ($Li_2C_6H_4O_4$) **96** were prepared by reacting the corresponding terephthalic and muconic acids $C_8H_6O_4$ **93** and $C_6H_6O_4$ **95** with $LiOH \cdot H_2O$ powder in 5 % excess in ethanol for 24 h (Scheme 21,

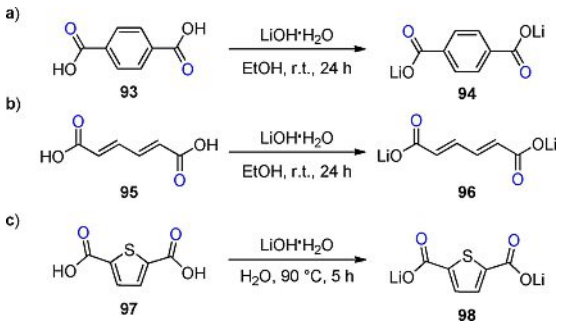

Scheme 21. Synthesis of a) *di*-lithium terephthalate ($Li_2C_8H_4O_4$) 94, b) *di*-lithium muconate ($Li_2C_6H_4O_4$) 96 and c) *di*-lithium thiophene-*2,5*- *di*-carboxylate (Li_2TDC) 98.

reactions a–b). Electrochemical tests versus Li of the compounds **94** and **96** were achieved using a 1.0 M $LiPF_6$ in EC/DMC (1/1 v/v) as the electrolyte and 30 wt.% carbon black. *Di*-lithium terephthalate ($Li_2C_8H_4O_4$) **94** and *di*-lithium muconate ($Li_2C_6H_4O_4$) **96** exhibited initial specific capacities of about 300 and 170 mAh·g^{-1}, respectively, which slowly decay to values of about 234 (78 % material activity) and 125 mAh·g^{-1} (36 % material activity) after 50 at a rate of 1 C, at an average cell potential of 0.8 V and 1.4 V *vs* Li/Li$^+$, respectively. In addition, the activity of both materials was maintained at 80 °C with PEO-based electrolytes.

Investigating excess capacity in π-conjugated carboxylates, *Lee et al.* studied also compounds **94** and **96**.[58] In addition, to support the effect of the cyclic structure on the excess capacity the *di*-lithium thiophene-*2,5-di*-carboxylate (**Li_2TDC**) **98**, was considered as heterocyclic *di*-carboxylate. The synthesis of the two compounds **94** and **96** were achieved following the procedure reported by Armand *et al.*[12e] For its part, **Li_2TDC 98** was prepared from thiophene-*2,5-di*-carboxylic acid **97** by deprotonation reaction with LiOH·H_2O in water at 90 °C for 5 h in 74% yield (Scheme 21, reaction c). Based on the insertion of one lithium ion per carboxylate group, the theoretical capacity of the *di*-lithium terephthalate **94** is 302 mAh·g^{-1}. When the $Li_2C_8H_4O_4$-based electrode was discharged to 0 V, a reduction plateau at 0.81 V and another sloping voltage plateau from 0.8 V to 0.0 V that gives a higher capacity (522 mAh·g^{-1}) equivalent to 3.5 lithium insertions, were observed after 15 cycles at 30 mA·g^{-1}. In contrast, compound **96**, with a linear open-chain-type π-conjugated geometry, exhibited a reversible discharge capacity of 241 mAh·g^{-1} after 50 cycles (corresponds to 1.4 lithium insertions) without any excessive lithiation and thus revealing the key role played by the aromatic core on the excess capacity of conjugated systems. In the case of the thiophene derivative **Li_2TDC 98** an exceptionally high discharge capacity of 850 mAh·g^{-1} equivalent to 5.8 lithium insertions was observed. Combining X-ray, isotope labelling, and solid state ^{13}C-NMR, the authors demonstrated that the abnormal excess capacity at low potential range below 0.7 V *vs* Li/Li^+ is due to the insertion of lithium ions into the internal structure of the cyclic compounds missing in the case of the linear compound, probably due to the structure conjugation break.

More recently, *Lakraychi et al.* investigated the substituent-effect on the electrochemical features of *di*-lithium di-substituted terephthalate derivatives evaluated in LIBs.[59] Different substituents showing distinct electronic effects were introduced to the *di*-lithium terephthalate ($Li_2C_8H_4O_4$) **94**. In this respect, bromo, methoxy and amino groups were considered. The synthesis of the three compounds *di*-lithium *2,5-di*-bromo-terephthalate **Li_2-DBT 101**, *di*-lithium *2,5-di*-methoxy-terephthalate **Li_2-DMoT 106** and *di*-lithium *2,5-di*-amino-terephthalate **Li_2-DAT 111** is detailed in Scheme 22. **Li_2-DBT 101** was obtained by $KMnO_4$-mediated oxidation reaction of compound **99** followed by lithiation reaction using hydrated LiOH in methanol (Scheme 22, reaction a). The synthesis of **Li_2-DMoT 106** was started by esterification reaction of compound **102** using $BF_3 \cdot Et_2O$ and CH_3OH. Methyl iodide was used to protect the two hydroxyl groups of the *di*-ester **103**. Ester **104** was hydrolysed with NaOH leading to the *di*-carboxylic acid **105** which was neutralized by hydrated LiOH to the desired molecule **Li_2-DMoT 106** (Scheme 22, reaction b). Amidification of *2,5-di*-methyl-*p*-phenyl-*di*-amine **107** using acetic anhydride and K_2CO_3 led to the protected compound **108**. $KMnO_4$-mediated oxidation reaction of the intermediate **108** afforded the *di*-carboxylic derivative **109**. Amide groups were hydrolysed using 10 wt.% solution of NaOH to afford the *di*-carboxylic acid **110** which was finally neutralized to the desired *di*-lithium *2,5-di*-amino-terephthalate **Li_2-DAT 111** (Scheme 22, reaction c). The electrochemical performances of the three *di*-lithium di-substituted terephthalate derivatives as cathodes active materials for rechargeable LIBs were studied using Li metal as the counter electrode. Composite electrodes were prepared by mixing the active material (**101**, **106** or **111**) with carbon Super P and PVdF binder in 60/30/10 wt.% and 1.0 M $LiPF_6$ solution in EC/DMC (1/1 v/v) was used as the electrolyte. The bromo derivative **Li_2-DBT 101** exhibited an initial capacity of 155 mAh·g^{-1} before fading to 122 mAh·g^{-1} after 50 cycles. However, **Li_2-DMoT 106** and **Li_2-DAT 111** delivered initial capacities of about 116 and 100 mAh·g^{-1}, respectively. Both showed only about 95 and 98 after 50 cycles, respectively. The authors attribute the capacity fading to the dissolution of the active materials or the steric hindrance of –OMe and –NH_2 groups. Interestingly, the studied terephthalate derivatives with strong inductive electron withdrawing effect (**–I**) and mesomeric electron donating effect (**+M**), show higher reduction potential values of 1.08 V for **Li_2-DBT 101**, 0.81 V for **Li_2-DMoT 106** and 0.75 V for **Li_2-DAT 111** *vs* Li/Li^+ compared to the previously studied *di*-lithium *2,5-di*-methyl terephthalate **Li_2-DMT**[60] with only electron-donating group (–CH_3) with a value of 0.65 V *vs* Li/Li^+. The authors thus demonstrated that the donor inductive effect groups could be desirable to design new Li carboxylate-based materials for low potential utilizations.

These materials paved the way to a new strategy to design organic active materials for LIBs where the carboxylate groups are not the only functional group contributing to the redox-

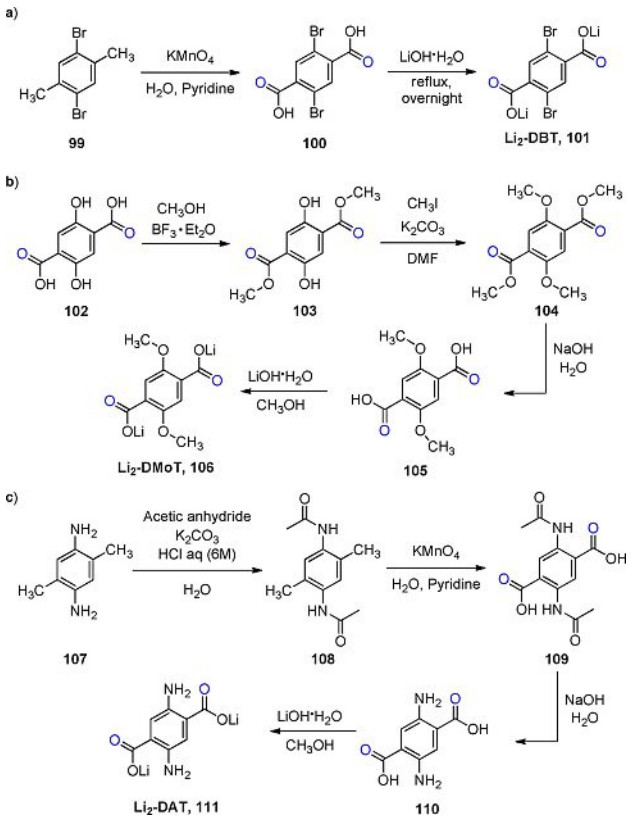

Scheme 22. Synthetic pathways towards a) *di*-lithium *2,5-di*-bromo-terephthalate Li_2-DBT 101, b) *di*-lithium *2,5-di*-methoxy-terephthalate Li_2-DMoT 106 and c) *di*-lithium *2,5-di*-amino-terephthalate Li_2-DAT 111.

activity. Recently, the 'superlithiation' mechanism has also been demonstrated by *Renault et al.* in *di*-lithium benzene-*di*-propiolate (**Li_2BDP**) **115** as a new material for LiBs.[61] The presence of the two carbon-carbon triple bonds segregates the carboxylate function from the aromatic centre without disruption of the conjugation during the lithiation. The **Li_2BDP 115** was prepared through the copper-free *Sonogashira* reaction using conditions adapted from *Park et al.*,[62] allowing a direct coupling of the electron-poor propiolic acid **113**, to *1,4-di*-iodobenzene **112** giving the benzene-*di*-propiolic acid (**H_2BDP**) **114** in 87% yield. The lithiation reaction with Li_2CO_3 afforded the desired compound **115** in 97% yield (Scheme 23). The **Li_2BDP 115** with

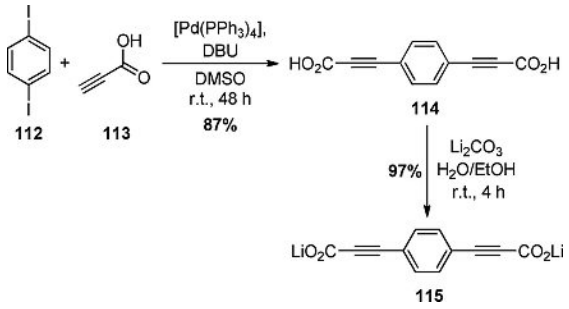

Scheme 23. Synthesis of *di*-lithium benzene-*di*-propiolate (Li_2BDP) 115. DMSO: *di*-methylsulfoxide.

50 wt.% carbon-based organic electrodes tested versus lithium metal using 1.0 M $LiPF_6$ in EC/DEC (1/1 v/v) as electrolyte exhibited the highest specific capacity for a lithium carboxylate (1363 $mAh \cdot g^{-1}$), with 11.5 lithium ions inserted per molecule. Density functional theory results emphasize that the reduction reaction starts by lithiation of the carbonyl groups, followed by the carbon-carbon triple bonds on the arms, while the high Li-loading led to the aromatic ring reduction.[61]

However, the 'superlithiation' mechanism of charge storage is a kinetically limited process and occurs at low operation voltage imposing restrictions for practical use. Accordingly, huge capacity differences are observed between some structurally-close compounds.[36a,63]

Another approach to increase the performance of organic electrode materials is the extension of the conjugated systems to enable π-stacking. For instance, *di*-lithium *4,4′*-tolane-*di*-carboxylate **119** was prepared by *Tarascon* and *co-workers* as active cathode material.[64] The one pot double *Sonogashira* Pd-catalyzed cross-coupling reaction between methyl-*4*-iodo-benzoate **116** and *tri*-methylsilyacetylene **117** gave the *di*-ester **118**. The *di*-ester **118** was then hydrolysed with KOH in water and ethanol. The acidification with HCl resulted in the corresponding *di*-carboxylic acid. Finally, the *di*-carboxylic acid was neutralized to the lithium salt using LiOH in ethanol resulting in the desired product **Li_2TDC 119** in 95.6% yield (Scheme 24). A LIB manufactured with **Li_2TDC 119** and 50 wt.% carbon black in 1.0 M $LiPF_6$ in EC/DMC (1/1 v/v) exhibited an initial capacity of ~200 $mAh \cdot g^{-1}$ at a cell potential of ~0.65 V *vs* Li/Li^+ corresponding to a lithium uptake of ~1.7 Li upon discharge. The capacity remained almost stable over 50 cycles at a rate of one

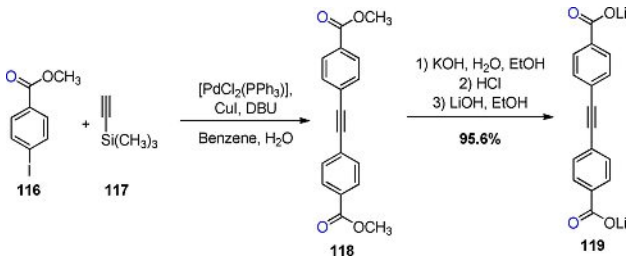

Scheme 24. Synthesis of *di*-lithium *4,4′*-tolane-*di*-carboxylate (Li_2TDC) 119.

Li per 20 h (0.025 C). The cell can be recharged to 76% of its full capacity at a charging rate of 2.5 C implying good rate capability.

Bécuwe and *co-workers* reported *di*-lithium *2,6*-naphthalene *di*-carboxylate (**Li_2-NDC**) **121**, as an anode material for LIBs.[65] The compound **121** has been synthesized starting from the corresponding acid (*2,6*-naphthalene *di*-carboxylic acid) **120** and LiOH using a freeze drying process which allowed superior electrochemical performances (Scheme 25). The electrode com-

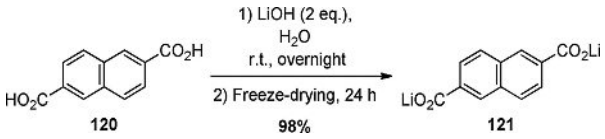

Scheme 25. Synthesis of *di*-lithium *2,6*-naphthalene *di*-carboxylate (Li_2-NDC) 121.

posed by active material **Li_2-NDC 121** (60 wt.%) mixed with 40 wt.% of carbon in 1.0 M $LiPF_6$ in EC/DMC (1/1 v/v) electrolyte, has a specific capacity of 176 $mAh \cdot g^{-1}$ at 1 C. The capacity retention of **Li_2-NDC 121** at 1 C rate decays before to stabilize at 115 $mAh \cdot g^{-1}$ after 50 cycles. At lower charging/discharging speed of 1 Li/20 h (0.025 C) the capacity dropped significantly to 20 $mAh \cdot g^{-1}$ (9% material activity) over 50 cycles indicating slow degradation of the active material into the electrolyte. Compared to the *di*-lithium terephthalate **94** (Scheme 21), **Li_2-NDC 121** showed a redox potential of 0.88 V *vs* Li/Li^+ 70 mV smaller that in *di*-lithium terephthalate **94**. Moreover, the extended conjugation of the naphthalene core provides higher rate capabilities.

In an effort to enhance the cycling performances of organic carboxylate electrodes, the hyper-conjugated perylene core unit was introduced between the lithium carboxylate groups to extend the intramolecular π-aromatic conjugation leading to a high stability of the radical anion. In this respect, *tetra*-lithium perylen-*3,4,9,10-tetra*-carboxylate (**Li_4-PTC**) **123** was studied as an anode active material by *Zhao et al.*,[66] and in another report by *Fédèle et al.*[67] The hydrolysis reaction of perylene-*3,4,9,10-tetra*-carboxylic acid *di*-anhydride **24** using KOH followed by an acidification reaction with H_2SO_4 led to perylene-*3,4,9,10-tetra*-carboxylic acid **122**. This latter was neutralized with LiOH in methanol to give the targeted **Li_4-PTC 123** (Scheme 26). The tested anodes were consisting of 70 wt.% **Li_4-PTC 123**, 10 wt.%

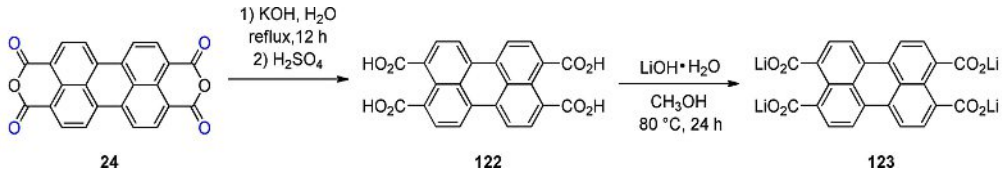

Scheme 26. Synthetic route of *tetra*-lithium perylen-*3,4,9,10-tetra*-carboxylate $Li_4C_{24}H_8O_8$ (Li_4-PTC) 123.

acetylene black,10 wt.% carbon black and 10 wt.% PTFE binder in 1.0 M $LiPF_6$ in EC/DMC/EMC (1/1/1 v/v/v) electrolyte. The **Li_4-PTC**-based electrode active material exhibited an initial capacity of ~200 $mAh \cdot g^{-1}$ (84% material activity) at 0.1 C at low charge/discharge plateaus of 1.20/1.10 V and remained stable over 100 cycles. In addition, stable capacities of 170 $mAh \cdot g^{-1}$ at 50 $mA \cdot g^{-1}$ and 110 $mAh \cdot g^{-1}$ at 400 $mA \cdot g^{-1}$, were obtained, respectively.

Recently, *Wang* and *co-workers* studied another type of organic salt containing azo group (–N=N–) for reversible lithiation/delithiation as a new family of organic electrode materials for LIBs.[68] Azobenzene **124** and methyl red sodium salt **125** were used as received. *4*-(phenyl-azo)-benzoic acid lithium salt (**PBALS**) **127** and azobenzene-*4,4′-di*-carboxylic acid lithium salt (**ADALS**) **130** were prepared by neutralizing the corresponding acids with LiOH (Scheme 27). Electrodes were consisting in azobenzene derivatives, carbon black and sodium alginate binder (or PVdF in the case of azobenzene) (60/30/10 wt.%). 6.0 M or 7.0 M LiTFSI in DOL/DME (1/1 v/v) was used as electrolyte and Li metal as the counter electrode. When cycled at 0.5 C, azobenzene **124** showed two charge/discharge plateaus at 2.5/1.9 V and 1.8/1.55 V, respectively, an initial capacity about 100 $mAh \cdot g^{-1}$ provided by the azo group as the active site. The specific capacity faded to about 60 $mAh \cdot g^{-1}$ with poor cycling stability due to its high solubility in the organic electrolyte. Despite the addition of sodium carboxylate group ($-CO_2Na$) at the *ortho* position to the azobenzene structure in compound **125**, no significant improvement of the electrochemical performance was observed. In contrast, better electrochemical performances were obtained when a Li carboxylate group was introduced at the *para* position of the *4*-(phenyl-azo) benzoic acid lithium salt (**PABLS**) **127**. Thus, two discharge plateaus at 1.47 and 1.25 V, and three charge plateaus at 1.30, 1.55, and 2.0 V were observed in agreement with the two cathodic peaks at 1.39 and 1.21 V, and the three anodic peaks at 1.33, 1.60, and 1.93 V monitored in the cyclic voltammograms. At 0.5 C rate, **PABLS 127** exhibited an initial capacity of 220 $mAh \cdot g^{-1}$ and a reversible capacity of 178 $mAh \cdot g^{-1}$ was retained after 100 cycles. To further improve the azobenzene derivative electrochemical properties and to supress the solubility issue, another Li carboxylate group was introduced in the aromatic structure of the azobenzene-*4,4′-di*-carboxylic acid lithium salt (**ADALS**) **130**. Two pairs of flat and long charge/discharge plateaus were observed at 1.5 and 1.55 V, respectively. **ADALS 130** delivered an initial capacity of 190 $mAh \cdot g^{-1}$ at 0.5 C, close to its theoretical capacity (190.1 $mAh \cdot g^{-1}$) and a reversible capacity of 175 $mAh \cdot g^{-1}$ was retained after 100 cycles with a coulombic efficiency close to 100% demonstrating superior electrochemical performance of **ADALS 130** in LIBs.

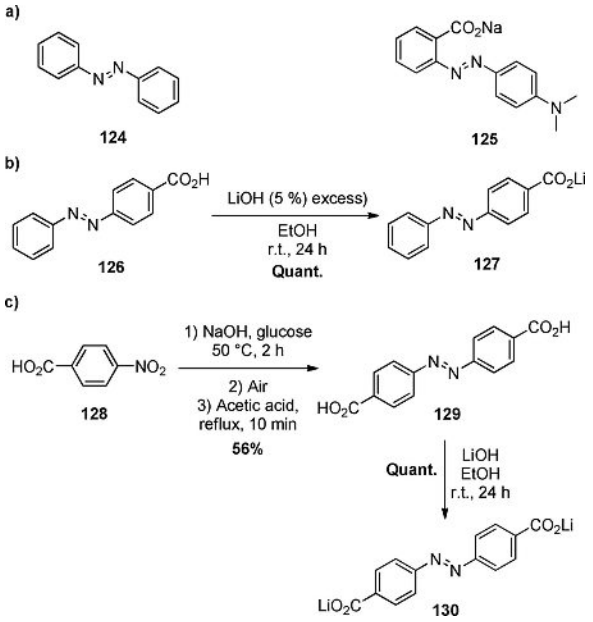

Scheme 27. a) Chemical structures of azobenzene 124 and methyl red sodium salt 125. Synthetic routes of b) *4*-(phenyl-azo) benzoic acid lithium salt (PABLS) 127 and c) azobenzene-*4,4′-di*-carboxylic acid lithium salt (ADALS) 130.

The good solubility of the π-conjugated aromatic molecules in organic electrolytes constitutes the biggest challenge for their application as the active materials in LIBs. Large efforts have been allocated to circumvent this problem by the introduction of large size molecular structures into the carbonyl-based aromatic skeletons or by formation of metal salts. An alternative approach to solve this problem is the incorporation of the carbonyl-based π-conjugated aromatic moieties into polymeric architectures, which is discussed in the next section.

Redox-Active Carbonyl-Based π-Conjugated Polymeric Structures for Li–Ion Batteries

Polymerization of organic electrode active materials is a widely used method to improve the cycling stability of organic batteries.[12h,16b,20a,27a,69] Energy and power sources consisting entirely (or mostly) of polymeric materials, the so-called "*Plastic Power*", offer several exciting opportunities for portable power devices such as lightweight, flexibility, higher viscosity (allowing

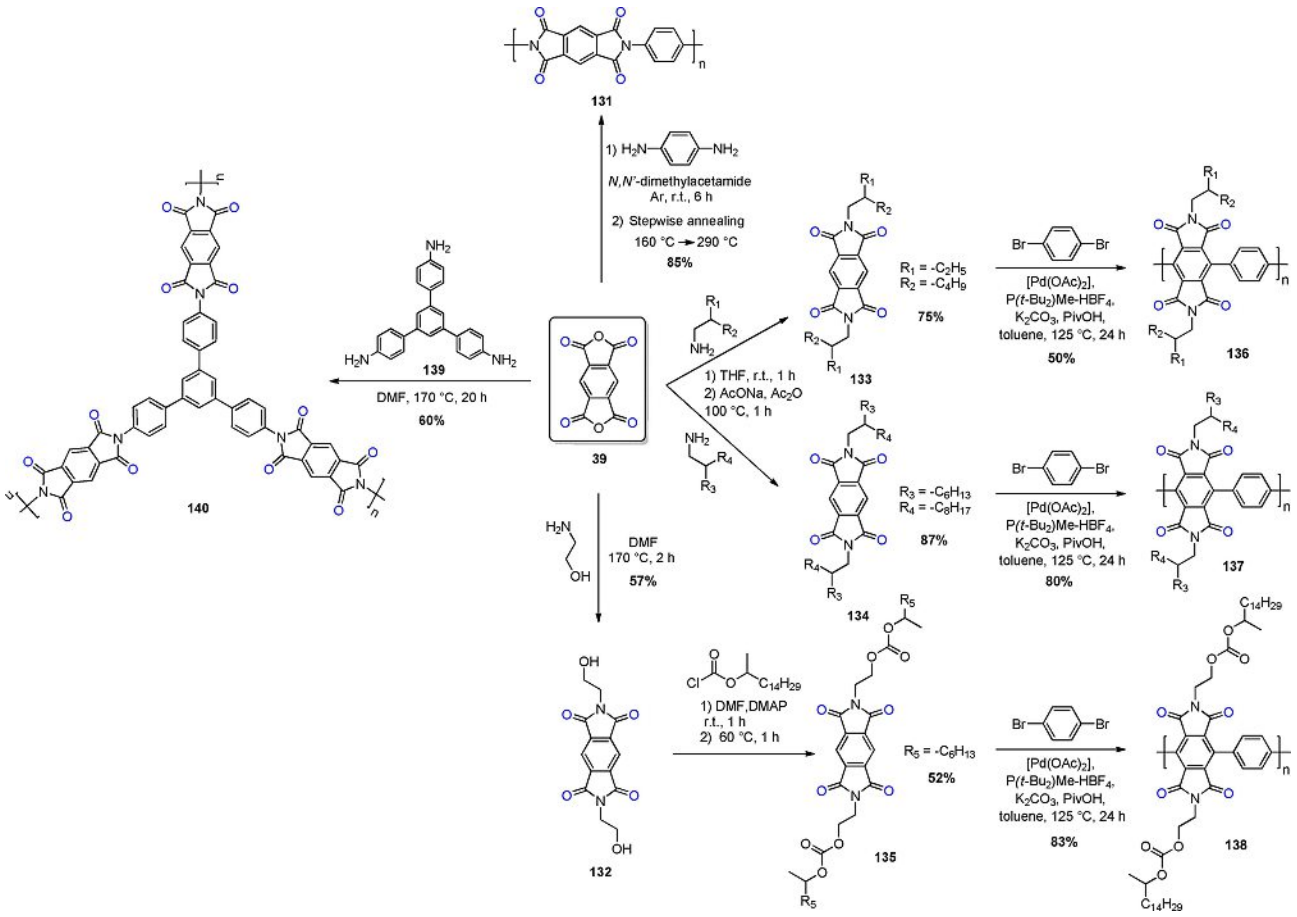

Scheme 28. Synthetic pathways towards PMDI-based polyimides 131, 136, 137, 138 and 140.

the reduction or even elimination of traditional binders), moldablility, processability redox stability or multi-electron reactions, just to name a few. Thanks to their mechanical properties, electro-active conjugated polymers could be bent, flexed, or even stretched.[17,70]

The first prototypes of commercial batteries with organic conductive polymers were launched in the late 1980s. *BASF* together with *VARTA* commercialized Li/polypyrrole battery and *Bridgestone* with *Seiko* tried the Li/polyaniline battery.[12f,g,71] Suffering from their inferior charge/discharge cycling behavior and sloping voltage, both were ceased after a short period. However, the discovery of carbonyl-based π-conjugated polymers with stable structures and poor solubility in organic electrolytes brought organic electrodes to the attention of the energy storage community. Thus, a great variety of redox-active polymers have been designed and investigated as electrode active materials for LIBs. In this context, polyimides[69a,72] and polyquinones[23b,73] constitute the main electro-active carbonyl-based π-conjugated polymers involved in energy storage applications.

Polyimides

Polyimides are known as important high performance engineering plastics with high thermal stability and good mechanical strength.[74] For example, **NDI**-based molecules continue to be one of the most widely studied materials in the organic electronics field, due to their electron affinity, redox behavior, good electron mobility, and light absorption.[75] Interestingly, the imide functional groups can undergo two one-electron reduction steps. The first fully reversible redox stage involves the reduction of phthalimides to the corresponding anion radicals and the second reduction step, irreversible, leads to the decomposition of the redox active structure.[20a] Despite that the aromatic imides can undergo redox-reactions, the research on the development of redox-active polyimides for electrochemical energy storage has been started only in 2010 simultaneously by *Nishide*[76] and *Zhou*[11b] groups. Since then, several different imide polymers have been studied as active materials in organic batteries.

Nishide and *co-workers* studied carbon nanocomposites of poly(pyromellitimido-*1,4*-phenylene) **131** as anode-active materials (Scheme 28).[76] Polymer **131** was prepared by a multistep annealing of the obtained polyamic acid through the polycondensation reaction of *p*-phenylenediamine and the corresponding pyromellitic *di*-anhydride **39** at r.t. in *N,N'-di*-methyl

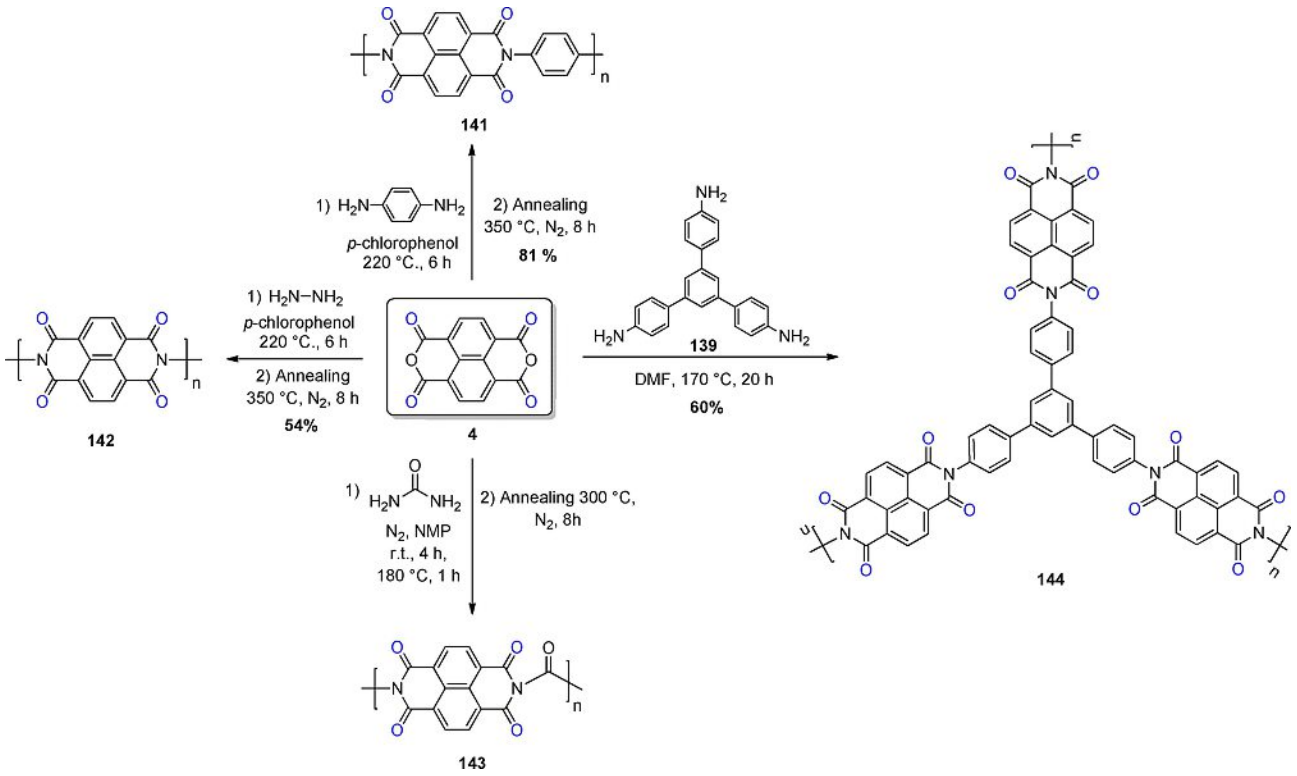

Scheme 29. Synthetic pathways towards NTCDI-based polyimides 141, 142, 143 and 144.

acetamide under argon atmosphere in 85% yield. The studied electrodes were consisting of the active material **131**, conductive VGCF and PVdF binder (5/85/10 wt.%) with 1.0 M solution of *tetra-n*-butylammonium perchlorate ($TBAClO_4$) in CH_3CN as electrolyte. An initial specific capacity of 95 $mAh \cdot g^{-1}$ at 0.03 C was obtained. Albeit the capacity was decreased to 70% after 10 cycles, the converged capacity exhibited excellent cyclability for more than 100 cycles without any further degradation.

A series of *N*-alkyl pyromellitic *di*-imide-based π-conjugated polyimides (**136**, **137** and **138**) were recently published by *Zindy et al.* as cathode active materials for LIBs applications.[77] *N*-alkyl-**PMDI**s were synthesized via direct hetero-arylation polymerization (DHAP) between their respective monomer with *1,4-di*-bromobenzene as co-monomer in the presence of palladium(II) acetate/*tri*-(*tert*-butylphosphonium) *tetra*-fluoroborate ([Pd$(OAc)_2$]/P(t-Bu_2)Me-HBF_4) as catalytic system, K_2CO_3 and pivalic acid (PivOH) in toluene at 125 °C for 24 h in 50%, 80% and 83% yields, respectively (Scheme 28). The composite electrodes were consisting in polymer, acetylene black and PVdF binder (30/60/10 wt.%) with 1.0 M solution of $LiPF_6$ in EC/DEC/DMC (1/1/1 v/v/v) as electrolyte. The three polymers **136**, **137** and **138** exhibited an initial discharge capacity of 33 $mAh \cdot g^{-1}$, 56 $mAh \cdot g^{-1}$ and 19 $mAh \cdot g^{-1}$ at low rate (0.05 C), respectively, at practical potential limits from 1.65 to 2.50 V *vs* Li/Li^+. Polyimide **137** with higher molar mass and longer side-chains (M_n = 31 kDa, hexyldecyl) showed a normalized capacity of 0.78 compared to the polymers **136** (M_n = 13 kDa, ethylhexyl) and **138** (M_n = 6 kDa, ethylhexyl), presenting normalized capacities of 0.32 and 0.25, respectively, and demonstrating the favourable effect of introducing longer alkyl side-chains onto the structures for battery stability and performance.

Simultaneously to the work of *Nishide*,[76] *Song et al.* prepared a series of carbonyl-based π-conjugated polyimides by polycondensation reaction using commercially available *1,4,5,8*-naphthalene *tetra*-carboxylic *di*-anhydride **4** with *di*-amine derivatives (*p*-phenylenediamine and hydrazine). The obtained polyimides **141** and **142** (Scheme 29) were used as cathode-active materials in rechargeable LIBs.[11b] The synthesis of both polymers **141** and **142** were achieved in refluxed *p*-chlorophenol as the solvent at 220 °C for 6 h followed by an annealing at 350 °C under N_2 atmosphere. Yields of 81% and 54% were obtained for polymers **141** and **142**, respectively. The cathodes, consisting of polyimide, conductive carbon and PTFE binder (60/30/10 wt.%), were tested using 1.0 M LiTFSI in DME/DOL (1/2 v/v) electrolyte and Li metal as counter electrode. The **141** and **142** polyimide-based cathode prototypes displayed initial capacities of about 163 and 202 $mAh \cdot g^{-1}$, respectively. After 100 cycles at a charging rate of 0.2 C capacities of 156 $mAh \cdot g^{-1}$ and 183 $mAh \cdot g^{-1}$ were still retained at a cell potential in the range of 2.0 to 2.5 V.

Using urea (carbonyl *di*-amine) and **NTCDA 4**, *Zhang* and *co-workers* investigated the electrochemical properties of naphthalene-based polyimide derivative **143** (Scheme 29) as cathode active-material for LIBs.[24a] Polymer **143** was synthesized through polycondensation of **NTCDA 4** with urea in NMP at 180 °C. The imidization was achieved by the ring closing dehydration at 300 °C under N_2 atmosphere (Scheme 29). The

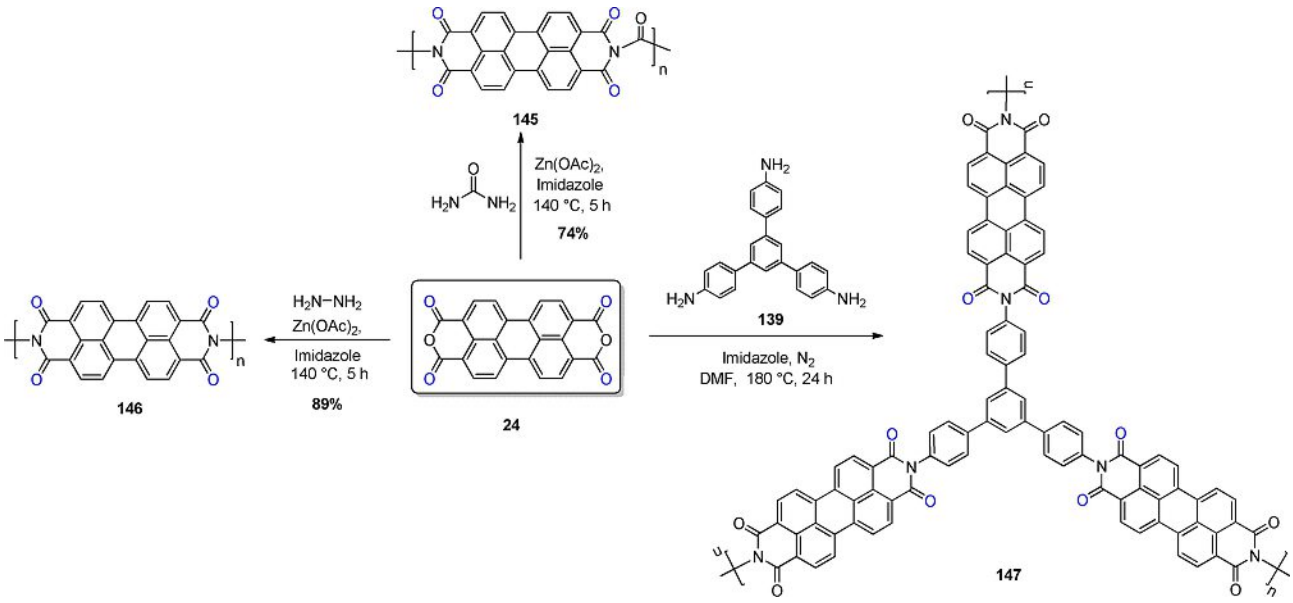

Scheme 30. Synthetic pathways towards PTCDI-based polyimides 145, 146 and 147.

polyimide **143** based electrode consisted of polymer **104**, carbon black and PVdF binder (60/10/30 wt.%). A 1.0 M $LiPF_6$ solution in EC/DMC (1/1 v/v) was used as electrolyte and Li metal was considered as counter electrode. The average reversible capacities of **143** were 175.4, 149.6 and 133.5 $mAh \cdot g^{-1}$ at 20, 50 and 500 $mA \cdot g^{-1}$, respectively. A good cycling stability and a capacity retention of 92% (153 $mAh \cdot g^{-1}$) could be obtained after 60 cycles at 50 $mA \cdot g^{-1}$. However, in a long-term cycling (150 cycles), the capacity of polymer **143** decreased gradually to 116 $mAh \cdot g^{-1}$.

Extending the aromatic system leads to a further stabilization of the radical anion, to a lower solubility of and higher conductivity within the active material due to π-π stacking, and to a lower theoretical capacity.[12i,20a] Therefore, perylene-polyimide-based polymers have been investigated as active electrode materials in LIBs. *Sharma et al.* reported the performance of polyimide derivatives of **PTCDA 145** and **146** (Scheme 30) as positive active materials for LIBs.[69a] The polymers **145** and **146** were synthesized through imidization of **PTCDA 24** using hydrazine and urea in the presence of zinc acetate ($Zn(OAc)_2$) and imidazole at 140 °C for 5 h generating products **145** and **146** in 89% and 74% yields, respectively. The two polymers showed plateaus near 2.5 V *vs* Li/Li^+ for both lithiation and delithiation with high CE (~100%). Stable capacity retention of 130 $mAh \cdot g^{-1}$ and 120 $mAh \cdot g^{-1}$ were obtained upon cycling up to 50 cycles at 50 $mA \cdot g^{-1}$ for the polymers **145** and **146**, respectively. It was found that the presence of additional carbonyl groups enhanced the conductivity upon cycling leading to good electrochemical performance in the case of polymer **145**.

In the same avenue, arylene *di*-imide-based polyimides frameworks were studied by *Tian et al.* as cathode active materials for LIBs.[78] Through condensation reactions of aromatic cross-linker *tri*-amine (*1,3,5*-tris(*4*-aminophenyl)-benzene, **TAPB**) **139** with a series of aromatic *di*-anhydrides; **PMDA 39** (Scheme 28), **NTCDA 4** (Scheme 29) and **PTCDA 24** (Scheme 30) were prepared. The synthesis of the three polymers **140**, **144** and **147** was conducted in DMF at high temperature (170–180 °C) in 60% ~70% yields. The working electrodes were composed of active material, acetylene black and PTFE binder (80/15/5 wt.%) using 1.0 M solution of $LiPF_6$ in EMC/EC/DMC (1/1/1 v/v/v) as electrolyte and Li metal as the counter electrode. The three polymers displayed initial discharge capacities of 61.7, 103.4 and 78.1 $mAh \cdot g^{-1}$ at a current density of 25 $mA \cdot g^{-1}$, respectively. The voltage remains constant at 2.35 V *vs* Li/Li^+. After 30 cycles, it dropped to 10, 68.5 and 70 $mAh \cdot g^{-1}$. A noticeable trend in capacity retention was observed, when increasing the size of the aromatic core, the capacity retention increases with **147** having better cyclability and capacity retention of 74.1% after 65 cycles.

Polyquinones

As for low molar mass *di*-imide-based molecules, small quinones suffer from serious solubility issues in organic electrolytes. To overcome the dissolution problem, quinones could be incorporated into a π-conjugated polymeric moiety. Despite that the electrochemical properties of quinoide-based polymers (quinone and anthraquinone) were first reported by *Manecke* and *Storck* several decades ago,[79] the development of alternative active electrode materials has revived the interest in quinone- and anthraquinone-containing polymers for LIBs during the past decade.

Simple polyquinone structures are of particular interest because they maintain the high specific capacity with high redox potential and can limit to a certain extent the solubility in the organic electrolytes. Poly(benzoquinonyl-sulfide) (**PBQS**)

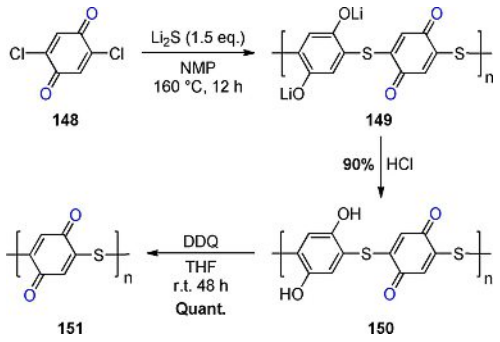

Scheme 31. Synthetic route of PBQS 151.

151, containing benzoquinone units linked by thioether bonds was examined by *Zhou* and *co-workers* as cathode for LIBs.[38] **PBQS 151** was synthesized by a polymerization-oxidation approach between *di*-chloro-benzoquinone **DCBQ 148** and an excess of lithium sulfide (Li_2S) at 160 °C in NMP affording the polymer **149** in a semi-reduced state. The acidification of **149** by HCl gave rise to the hydroquinone polymer **150** in 90% yield. The final **PBQS 151** was obtained by the quantitative oxidation reaction of the polymer **150** using **DDQ** (Scheme 31). The tested cathode was consisting of **PBQS 151**, carbon and PTFE binder (60/30/10 wt.%) with 1.0 M solution of LiTFSI in DME/DOL (1/1 v/v) was utilized as electrolyte and Li metal as the counter electrode. **PBQS 151** exhibited an initial capacity of 232 $mAh \cdot g^{-1}$ at 50 $mA \cdot g^{-1}$ with 74% retention after 100 cycles and an average discharge voltage of 2.67 V *vs* Li/Li^+. A specific capacity of 198 $mAh \cdot g^{-1}$ at 5000 $mA \cdot g^{-1}$ with stable long-term cycling performance (86% capacity retention after 1000 cycles at 500 $mA \cdot g^{-1}$) and a high CE of 99.5% were observed.

In a similar spirit, the same group investigated the poly(*2,5-di*-hydroxy-*p*-benzoquinonyl-sulfide) (**PDHBQS**) **153** and its corresponding lithium salt (**Li_2PDHBQS**) **154** as active materials for LIBs.[80] The **Li_2PDHBQS 154** was prepared from chloranilic acid **152** in 85% yield following the procedure used for the polymer **149**. The acidification of polymer **154** led to poly(*2,5-di*-hydroxy-*p*-benzoquinonyl-sulfide) (**PDHBQS**) **153** in 54% yield (Scheme 32). The investigated cathodes were consisting of

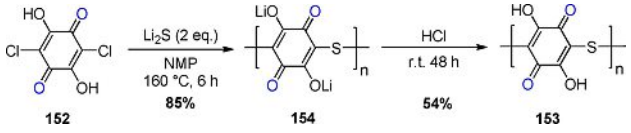

Scheme 32. Synthesis of Li_2PDHBQS 154 and PDHBQS 153.

PDHBQS 153 or **Li_2PDHBQS 154**, carbon and PTFE binder (60/30/10 wt.%) using 1.0 M solution of LiTFSI in DME/DOL (1/1 v/v) as electrolyte and Li metal as the counter electrode. **PDHBQS 153** exhibits an initial capacity of 228 $mAh \cdot g^{-1}$ (78% active material) at 50 $mA \cdot g^{-1}$ with sloping charge/discharge curves at a cell potential between 2.35 and 1.75 V. However, the capacity faded to 100 $mAh \cdot g^{-1}$ after 20 cycles. The lithiated derivative **Li_2PDHBQS 154** showed an initial capacity of 268 $mAh \cdot g^{-1}$

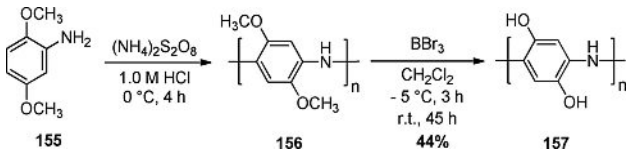

Scheme 33. Synthesis of poly(*2,5-di*-hydroxyaniline) 157.

(93% material activity) at 50 $mA \cdot g^{-1}$ with a high rate capability and cycling stability attested by a capacity retention of about 90% after 1500 cycles at 500 $mA \cdot g^{-1}$.

Vlad and *co-workers* reported the use of poly(*2,5-di*-hydroxyaniline) **157** as cathode active material for LIBs.[81] The active redox material **157** was obtained by oxidative polymerization of *2,5-di*-methoxyaniline monomer **155** using ammonium persulfate ($(NH_4)_2S_2O_8$) followed by BBr_3-assisted de-methylation of poly(*2,5-di*-methoxyaniline) **156** affording the desired hydroquinone polymer **157** in 44% yield (Scheme 33). Polymer **157** displays an intrinsic electrical conduction along the polyaniline-type backbone and quinone-like redox activity with a theoretical energy storage capacity of 443 $mAh \cdot g^{-1}$. The investigated electrode formulation was consisting in polymer **157**, carbon and PVdF binder (60/30/10 wt.%) and 1.0 M $LiPF_6$ in EC/DEC (1/1 v/v) used as electrolyte, while Li metal was employed as counter electrode. Polymer **157** with a maximum de-methylation extent evidenced by a decreased C/N atomic ratio (6) displayed an open circuit potential in the range of 2.8–3.2 V *vs* Li/Li^+ and an initial capacity of 270 $mAh \cdot g^{-1}$ at 0.1 C. However, a poor cycling stability with only 7% capacity retention was observed after 5 cycles, assigned to an irreversible keto-enol tautomerism of the hydroxyl groups linked to the quinoids groups.

Besides benzoquinone polymers, anthraquinone-based polymers have also been investigated as cathodes for LIBs. Poly(*5*-amino-*1,4-di*-hydroxy-anthraquinone) **159** was investigated by *Zhao et al.* as cathode material in a lithium-organic battery.[23b] The polymer **159** was synthesized by oxidative polymerization of *5*-amino-*1,4-di*-hydroxy-anthraquinone **158** in the presence of $(NH_4)_2S_2O_8$ in glacial acetic acid at −5 °C for 4 h (Scheme 34). Composite electrodes were prepared with **159**, acetylene black and PVdF binder (50/40/10 wt.%). A 1.0 M solution of $LiPF_6$ in EC/DEC (1/1 v/v) was used as electrolyte and Li metal as the counter electrode. At the cutoff voltage of 1.5–3.7 V, polymer **159** showed the initial discharge capacity of 101 $mAh \cdot g^{-1}$ at the current density of 400 $mA \cdot g^{-1}$. The capacity increases to 143 $mAh \cdot g^{-1}$ during the first 14 cycles ascribed to the gradual

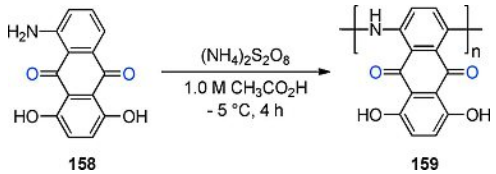

Scheme 34. Synthetic route to poly(*5*-amino-*1,4-di*-hydroxy anthraquinone) 159.

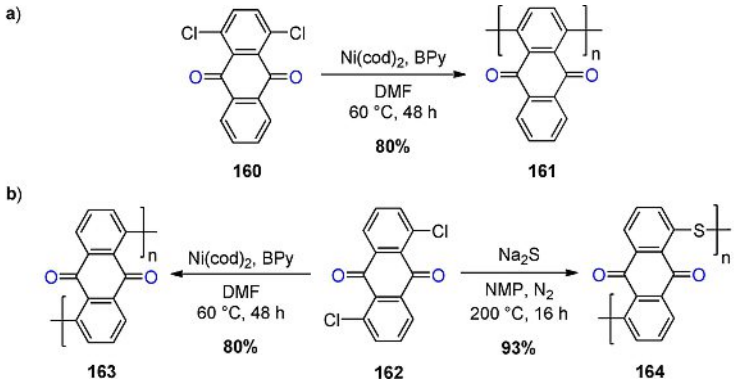

Scheme 35. Synthetic route to anthraquinone-based polymers 161, 163 and 164.

increase amount of doping ions in the polymer chains. After 50 cycles, the specific capacity was maintained at 129 mAh·g^{-1} illustrating good cycling performance.

Song et al. polymerized different isomers of anthraquinone namely, *1,4-di*-chloroanthraquinone **160** or *1,5-di*-chloroanthraquinone **162** as monomers with either a Ni-catalysed polycondensation reaction or using sulphur forming poly(*1,4*-anthraquinone) **161**, poly(*1,5*-anthraquinone) **163** or poly(*1,5*-anthraquinonyl sulfide) **164**. The obtained polymers were investigated as organic cathode active materials for rechargeable LIBs.[19b,38] The Ni-catalysed polymerization reaction was conducted in DMF at 60 °C using bis(*1,5*-cyclooctadiene)nickel (0) (Ni(cod)$_2$) and *2,2′*-bipyridine (BPy) as ligand affording polymers **161** and **163** in 80% yield. In the other hand, *Phillips* method using sodium sulfide (Na_2S) allowed the preparation of the anthraquinone sulfide polymer **164** in 93% yield (Scheme 35). The cathode films were composed of active material (**161** or **163**), carbon and PTFE binder (60/30/10 wt.%) for electrochemical characterization. A 1.0 M LiTFSI in DOL/DME (2/1 v/v) was used as electrolyte and Li metal as counter electrode. A battery equipped with polymer **161** composite electrode exhibited an initial capacity of 263 mAh·g^{-1} at a current rate of 0.2 C. After 1000 cycles, the capacity retention was 98% (248 mAh·g^{-1}) and 99% (235 mAh·g^{-1}) at current rates of 1 C and 2 C, respectively. Furthermore, 69% of the capacity was retained (180 mAh·g^{-1}) at a current rate of 20 C over 140 cycles, demonstrating a stable cycling performance. The polymer **163** electrode with low molecular weight (*ca.* 2300 Da for **163** *vs ca.* 230000 Da for **161**) delivered an initial capacity of about 230 mAh·g^{-1} at a current rate of 0.2 C. A capacity retention of only 68% (~163 mAh·g^{-1}) was obtained after 100 cycles due to its solubility in the electrolyte. In the other hand, the studied electrode was composed of polymer **164**, acetylene black and PTFE binder (40/40/20 wt.%) with 1.0 M solution of LiTFSI in DOL/DME (1/1 v/v) as electrolyte and Li metal as counter electrode. The battery showed an initial discharge capacity of 198 mAh·g^{-1} at 50 mA·g^{-1} corresponding to 88% of its theoretical value (225 mAh·g^{-1}). The capacity faded to 178 mAh·g^{-1} (79% material activity) over 200 cycles at the same current rate. When a current density of 500 mA·g^{-1} was applied, a capacity of 151 mAh·g^{-1} (79% material activity) was maintained.

Recently, *Petronico et al.* developed a lithium salt polymer of *di*-hydroxyanthraquinone (poly(*di*-hydroxyanthraquinonyl sulfide) (**P(LiDHAQS)**) **166** capable of storing four Li^+ per monomer.[82] The synthesis of polymer **166** was carried out using a modified *Philips* method: *5,8-di*-chloro-*1,4-di*-hydroxyanthraquinone **165** reacted with Li_2S in NMP under N_2 atmosphere at 160 °C for 18 h giving the **P(LiDHAQS) 166** polymer in 90% yield (Scheme 36). The studied composite cathodes were consisting in **P(LiDHAQS) 166** polymer and conductive carbon

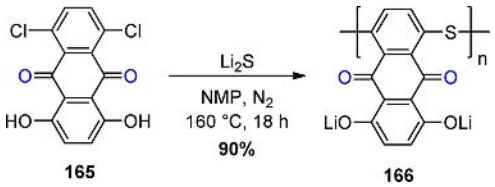

Scheme 36. Synthesis of P(LiDHAQS) 166.

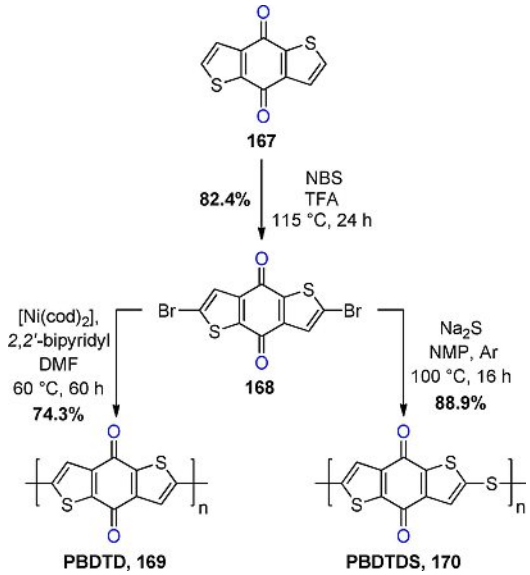

Scheme 37. Synthetic routes for PBDTD 169 and PBDTDS 170.

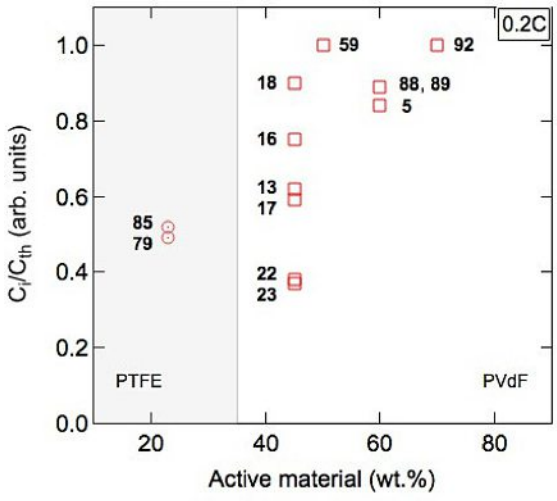

Figure 3. For the two most used binders, PTFE (open circles) and PVdF (open squares), C_i/C_{th} (arb. units), at 0.2 C discharge rate, is plotted at the indicated active material load (wt.%).

(50/50 wt.%) mixed with PTFE (10 wt.%) binder. For electrochemical performance assessment, 1.0 M LiTFSI in DOL/DME (2/1 v/v) was used as electrolyte and Li metal as counter electrode. Half-cells of **P(LiDHAQS) 166** showed an initial discharge capacity of 300 mAh·g^{-1} at a rate of 2 C. Then, the capacity decayed to stabilize at 210 mAh·g^{-1} after 1200 cycles with an average discharge voltage of 2.5 V *vs* Li/Li$^+$. Finally, the polymer was able to store only 3.5 Li$^+$ per monomer less than the ideal 4 Li$^+$ capacity likely because of the intrinsically poor electrical conductivity of the material.

In a later work by *Yao* and *co-workers*, π-conjugated oligomeric hetero-aromatic-fused quinones, poly(benzo[*1,2-b:4,5-b′*]*di*-thiophene-*4,8-di*-one-*2,6*-diyl) (**PBDTD**) **169** and poly(benzo[*1,2-b:4,5-b′*]*di*-thiophene-*4,8-di*-one-*2,6*-diyl sulfide) (**PBDTDS**) **170**, with two different molecular conformations (planar in PBDTD and helical in PBDTDS) were designed and investigated in Li-ion storage systems (Scheme 37).[83] The synthesis of BDTD-based polymers **130** and **131** was started by the preparation of the *2,6-di*-bromobenzo[*1,2-b:4,5-b′*]*di*-thiophene-*4,8-di*-one (**Br_2BDTD**) **168** monomer starting from benzo[*1,2-b:4,5-b′*]*di*-thiophene-*4,8-di*-one (**BDTD**) **128** using *N*-bromo-succinimide (NBS) in refluxed TFA for 24 h. **PBDTD 169** was obtained by Ni-catalyzed poly-condensation reaction of **Br_2BDTD 168** using *bis*(*1,5*-cyclooctadiene) nickel(0) (Ni(cod)$_2$) and *2,2′*-bipyridyl as ligand in dry DMF at 60 °C. The synthesis of **PBDTDS 170** was achieved in NMP by reacting **Br_2BDTD 168** with Na_2S under Ar-atmosphere at 100 °C for 16 h. Composite electrodes containing active material (**169** or **170**) and 19.1 wt.% CNTs were studied as cathodes using Li metal as counter electrode and 1.0 M $LiClO_4$ in DOL/DME (1/1 v/v) as electrolyte. **PBDTD 169** and **PBDTDS 170** exhibited initial specific capacities of about 214 and 200 mAh·g^{-1} at 5 C rate, at an average cell potential of 2.52 V and 2.56 V *vs* Li/Li$^+$, respectively. **PBDTD 169** exhibited 96% of capacity retention after 250 cycles, while **PBDTDS 170** showed an increase of capacity from 121 to 145 mAh·g^{-1} during the 50 first cycles and stabilized at 137 mAh·g^{-1} after 250 cycles. These results have to be compared to the poly(*2*-vinylbenzo[*1,2-b:4,5-b′*]-*di*-thiophene-*4,8-di*-one) (**PVBDT**) containing pendant **BDTD** units reported by *Schubert* and *co-workers*,[84] which showed 15–54% capacity retention after 100 cycles albeit containing 50–80 wt.% of CNTs conductive additive.

Conclusion

Owing to their lightweight, easy chemical modification, and ability to undergo multiple redox reaction, carbonyl-based redox-active materials are perceived as auspicious electrode materials for energy storage systems. Therefore, they have gained significant attention during the last decades. In this review, we have integrated the state of the art of synthetic strategies followed to prepare various functional carbonyl-based π-conjugated compounds applied as electrodes for LIBs. From the recent studies on the carbonyl-based π-conjugated active materials family, including low molecular weight molecules and polymers, it has been demonstrated that these

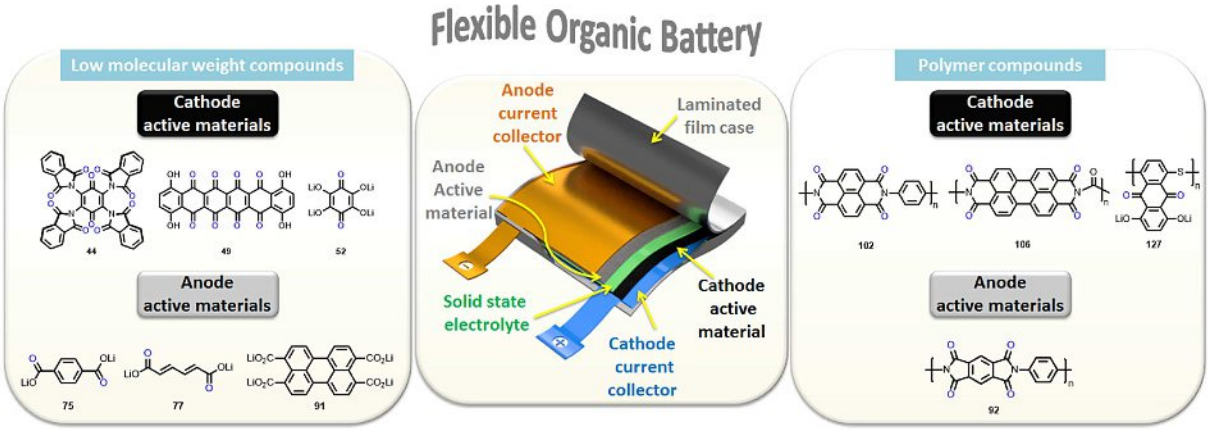

Figure 4. Schematic representation of a flexible battery with some examples of carbonyl-based π-conjugated compounds, which could be exploited as redox-active materials for all-organic rechargeable lithium batteries.

Table 1. Overview of electrochemical performance of related carbonyl-based π-conjugated electrode materials. The description includes, for each material, the synthetic method, the electrolyte, the electrode composition [wt.%] (active material/conductive additive/binder), the conducting additive, the binder, the theoretical capacity C_{th} [mAh·g^{-1}], the initial discharge capacity C_i [mAh·g^{-1}] and rate [reported with respect to 1 C], the rated capacity C_n [mAh·g^{-1}] and cycle number, the potential [V], and the reference work. Here n.r. denotes a value not reported.

Materials	Method	Electrolyte	Electrode (active material/ conductive additive/binder) [wt.%]	Additive	Binder	C_{th} [mAh·g^{-1}]	C_i [mAh·g^{-1}], rate	C_n [mAh·g^{-1}], Cycle number	Potential [V]	Ref.
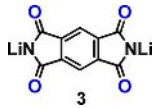 3	Lithiation	1.0 M LiTFSI, DMC	66/34	Carbon SP	–	236	220, 0.025	200, 20	1.81, 1.62	26
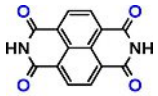 5	Condensation	1.0 M LiTFSI DOL/ DME (1/1 v/v)	60/30/10	Carbon black	PVdF	201	170, 0.2	34, 10	2.52	27c
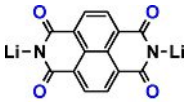 6	Lithiation	1.0 M LiTFSI, DOL/ DME (1/1 v/v)	60/30/10	Carbon black	PVdF	192	131, 0.5	117, 100	2.32	27c
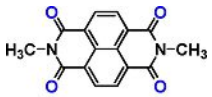 7	Condensation	1.0 M LiTFSI, DOL/ DME (1/1 v/v)	60/30/10	Carbon black	PVdF	182	167, 0.5	20, 40	2.5	27c
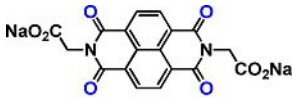 10	Condensation	1.0 M $LiPF_6$, EC/DMC (1/1 v/v)	70/30	Carbon black	-	125	157, 0.1	147, 50	2.5	32
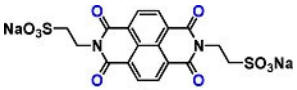 11	Condensation	1.0 M $LiPF_6$, EC/DMC (1/1 v/v)	70/30	Carbon black	–	102	117, 0.1	113, 50	2.5	32
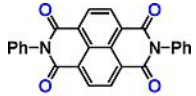 12	Condensation	1.0 M $LiPF_6$, EC/EMC/ DMC (1/1/1 v/v/v)	50/40/10	Acetylene black	PVdF	256	170, 0.1	119, 100	2.1, 2.3	33
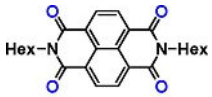 13	Condensation	1.0 M $LiClO_4$, EC/DMC (1/1 v/v)	45/50/5	Acetylene black	PVdF	123	76, 0.2	92, 10	2.5	27b
 16	Condensation/ Aryl substitution	1.0 M $LiClO_4$, EC/DMC (1/1 v/v)	45/50/5	Acetylene black	PVdF	103	77, 0.2	41, 10	2.3	27b

Table 1. continued

Materials	Method	Electrolyte	Electrode (active material/ conductive additive/binder) [wt.%]	Additive	Binder	C_{th} [mAh·g^{-1}]	C_i [mAh·g^{-1}], rate	C_n [mAh·g^{-1}], Cycle number	Potential [V]	Ref.
 17	Condensation/Aryl substitution	1.0 M $LiClO_4$, EC/DMC (1/1 v/v)	45/50/5	Acetylene black	PVdF	114	67, 0.2	45, 10	2.6	27b
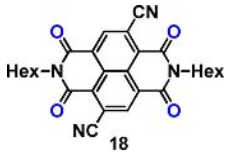 18	Condensation/ Aryl substitution	1.0 M $LiClO_4$, EC/DMC (1/1 v/v)	45/50/5	Acetylene black	PVdF	111	100, 0.2	80, 10	2.8	27b
 22	Condensation/ Aryl substitution	1.0 M $LiClO_4$, EC/DMC (1/1 v/v)	45/50/5	Acetylene black	PVdF	170	64, 0.2	34, 10	2.9	27b
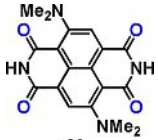 23	Condensation/ Aryl substitution	1.0 M $LiClO_4$, EC/DMC (1/1 v/v)	45/50/5	Acetylene black	PVdF	152	57, 0.2	30, 10	2.4	27b
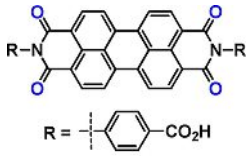 25, Benzoic-PDI	Condensation	1.0 M $LiPF_6$, EC/DEC (1/1 v/v)	60/30/10	Acetylene black	Kynar	85	104, 5	75, 200	2.7	28a
 27	Commercial	1.0 M $LiPF_6$, EC/DEC/ PC (4/5/1 v/v/v)	60/30/10	Ketjen black	PTFE	137	123, 0.5	119, 200	2.75	28b

Table 1. continued

Materials	Method	Electrolyte	Electrode (active material/ conductive additive/binder) [wt.%]	Additive	Binder	C_{th} [mAh·g^{-1}]	C_i [mAh·g^{-1}], rate	C_n [mAh·g^{-1}], Cycle number	Potential [V]	Ref.
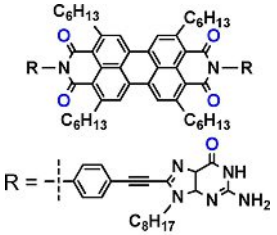 G_2PDI 38	Sonogashira cross coupling	1.0 M $LiPF_6$, EC/DMC (1/1 v/v)	80/10/10	Carbon black	PVdF	37	27, 0.05	25, 300	1.8, 2.3	34
 24	Commercial	1.0 M $LiPF_6$ EC/DMC (1/1 v/v)	80/15/5	Acetylene black	PTFE	273	131, 0.5	65, 80	2.4	22
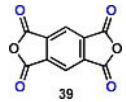 39	Commercial	1.0 M $LiClO_4$, PC	60/40	Acetylene black	–	246	n.r.	n.r.	3.1, 3.2	35
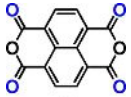 4	Commercial	1.0 M $LiPF_6$, EC/DMC (1/1 v/v)	60/35/5	Acetylene black	PTFE	1800	1804, 0.1	900, 30	2.34, 1.69, 1.04, 0.47	36
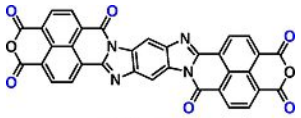 NDA-4N, 44	Condensation	1.0 M LiTFSI, DOL/ DME (1/1 v/v) 1 % $LiNO_3$	30/50/20	CNT	PVdF	178	142, 0.33	49, 99	2.4	37
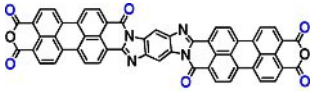 PDA-4N, 48	Condensation	1.0 M LiTFSI, DOL/ DME (1/1 v/v) 1 % $LiNO_3$	30/50/20	CNT	PVdF	126	116.3, 0.33	82, 99	2.4	37
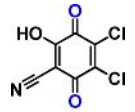 53	Hydrolysis	1.0 M $LiPF_6$, EC/DMC (1/1 v/v)	30/60/10	Carbon SP	PTFE	1010	2275, n.r.	1009, 50	1.6–1.0	40
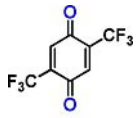 58a	Cu-catalysed per-fluoro-alkylation	1.0 M $LiPF_6$, EC/DEC (3/7 v/v)	3/87/10	VGCF	PTFE	220	162, n.r.	60, 20	3.0	42

Table 1. continued

Materials	Method	Electrolyte	Electrode (active material/ conductive additive/binder) [wt.%]	Additive	Binder	C_{th} [mAh·g^{-1}]	C_i [mAh·g^{-1}], rate	C_n [mAh·g^{-1}], Cycle number	Potential [V]	Ref.
 58b	Cu-catalysed per-fluoro-alkylation	1.0 M $LiPF_6$, EC/DEC (3/7 v/v)	3/87/10	VGCF	PTFE	99	115, n.r.	58, 20	3.0	42
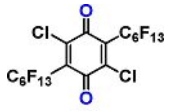 58c	Cu-catalysed per-fluoro-alkylation	1.0 M $LiPF_6$, EC/DEC (3/7 v/v)	3/87/10	VGCF	PTFE	66	177, n.r.	98, 20	3.1	42
 59	Nucleophilic substitution	1.0 M LiTFSI, DOL/ DME (1/1 v/v)	50/40/10	Carbon SP	PVdF	233	223.2, 0.2	204, 100	2.8	44
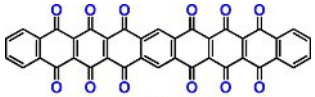 62	Condensation	1.0 M $LiClO_4$, PC/DME (1/1 v/v)	30/40/20	Carbon black	PTFE	489	125, 0.5	115, 0.5 C	3.0	46
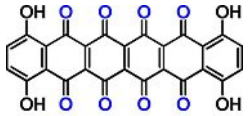 64	Condensation	1.0 M $LiPF_6$, EC/DEC (1/1 v/v)	50/45/5	Acetylene black	PVdF	628	340, n.r.	203, 40	2.7	48
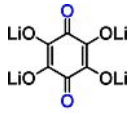 67	Disproportionation or Lithiation	1.0 M $LiPF_6$, EC/DMC (1/1 v/v)	80/20	Ketjen black	–	274	200, 1	170, 50	1.8	49
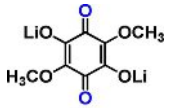 70	Nucleophilic substitution + Lithiation	1.0 M $LiPF_6$ EC/DMC (1/1 v/v)	57/[33/10]	Carbon SP/ γ-Al_2O_3	–	253	136, 0.16	80, 50	3.1	50
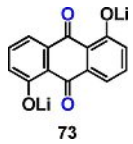 73	Lithiation	1.0 M $LiPF_6$, EMC/EC/ DMC (1/1/1 v/v/v)	60/15/5	Acetylene black	PTFE	212	115, 0.5	100, 50	1.75	54

Table 1. continued

Materials	Method	Electrolyte	Electrode (active material/ conductive additive/binder) [wt.%]	Additive	Binder	C_{th} [mAh·g^{-1}]	C_i [mAh·g^{-1}], rate	C_n [mAh·g^{-1}], Cycle number	Potential [V]	Ref.
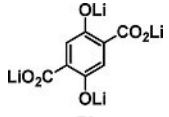 76	Lithiation + Annealing	1.0 M $LiPF_6$, EC/DMC (1/1 v/v)	65/30/5	Carbon black	PVdF	241	223, 0.1	211, 50	2.8	14b
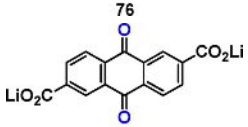 79	Nucleophilic substitution + Lithiation	1.0 M $LiPF_6$, PC	23/62/15	Acetylene black	PTFE	174	85, 0.2	85, 20	1.7	55
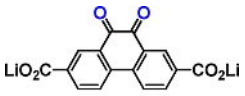 85	Nucleophilic substitution + Lithiation	1.0 M $LiPF_6$, PC	23/62/15	Acetylene black	PTFE	174	90, 0.2	95, 20	2.1	55
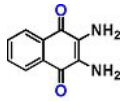 88	Nucleophilic substitution + Hydrolysis	1.0 M LiTFSI, DME/ DOL (1/2 v/v)	60/30/10	Carbon SP	PVdF	281	250, 0.2	248, 500	2.33, 2.41	56
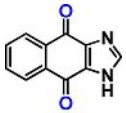 89	Condensation	1.0 M LiTFSI, DME/ DOL (1/2 v/v)	60/30/10	Carbon SP	PVdF	270	240, 0.2	152, 100	2.48, 2.57	56
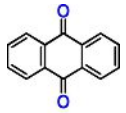 90	Commercial	1.0 M $LiPF_6$, DMC	70/20/10	Acetylene black	PVdF	257	270, 0.1	40, 100	2.1	57
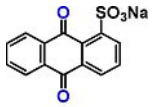 91	Commercial	1.0 M $LiPF_6$, DMC	70/20/10	Acetylene black	PVdF	173	137, 0.1	75, 100	2.25	57
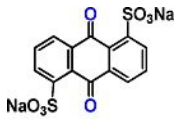 92	Commercial	1.0 M $LiPF_6$, DMC	70/20/10	Acetylene black	PVdF	130	130, 0.2	120, 100	2.4	57
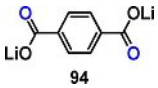 94	Lithiation	1.0 M $LiPF_6$, EC/DMC (1/1 v/v)	70/30	Carbon black	–	302	300, n.r.	234, 50	0.85	12e

Table 1. continued

Materials	Method	Electrolyte	Electrode (active material/ conductive additive/binder) [wt.%]	Additive	Binder	C_{th} [mAh·g^{-1}]	C_i [mAh·g^{-1}], rate	C_n [mAh·g^{-1}], Cycle number	Potential [V]	Ref.
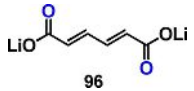 96	Lithiation	1.0 M $LiPF_6$, EC/DMC (1/1 v/v)	70/30	Carbon black	–	349	170, n.r.	125, 50	1.4	12e
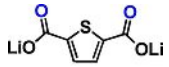 98	Lithiation	0.8 M $LiPF_6$, EC/DEC (1/1 v/v)	50/37.5/12.5	Carbon SP	CMC	292	850, n.r.	n.r.	1.0	58
 Li_2-DBT, 101	Oxidation + Lithiation	1.0 M $LiPF_6$, EC/DMC (1/1 v/v)	60/30/10	Carbon SP	PVdF	155	155, n.r.	122, 50	1.01	59
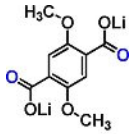 Li_2-DMoT, 106	Lithiation	1.0 M $LiPF_6$, EC/DMC (1/1 v/v)	60/30/10	Carbon SP	PVdF	225	116, n.r.	95, 50	0.81	59
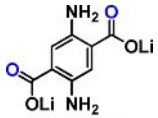 Li_2-DAT, 111	Oxidation + Lithiation	1.0 M $LiPF_6$, EC/DMC (1/1 v/v)	60/30/10	Carbon SP	PVdF	257	100, n.r.	98, 50	0.75	59
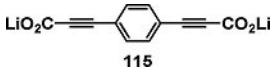 115	Sonogashira cross coupling + Lithiation	1.0 M $LiPF_6$, EC/DEC (1/1 v/v)	50/50	Carbon SP	-	118	1363, n.r.	200 (at 1 Li^+/ 5), 100	0.4, 1.1, 2.2, 2.9	61
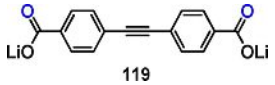 119	Sonogashira cross coupling + Lithiation	1.0 M $LiPF_6$, EC/DMC (1/1 v/v)	50/50	Carbon SP	–	192	200, 0.025	195, 50	0.7	64
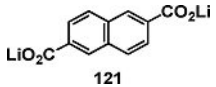 121	Lithiation	1.0 M $LiPF_6$, EC/DMC (1/1 v/v)	66/33	Carbon black	–	235	176, 1	115, 50	0.88	65
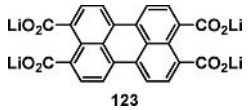 123	Hydrolysis + Lithiation	1.0 M $LiPF_6$, EC/DMC/ EMC (1/1/1 v/v/v)	70/20/10	Carbon black, Acetylene black	PTFE	237	200, 0.1	200, 1200	1.1	66
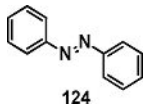 124	Commercial	6.0 M LiTFSI, DOL/ DME (1/1 v/v)	60/30/10	Carbon black	PVdF	294	100, 0.5	60, 20	1.9, 1.55	68a

Table 1. continued

Materials	Method	Electrolyte	Electrode (active material/conductive additive/binder) [wt.%]	Additive	Binder	C_{th} [mAh·g^{-1}]	C_i [mAh·g^{-1}], rate	C_n [mAh·g^{-1}], Cycle number	Potential [V]	Ref.
125	Commercial	6.0 M LiTFSI, DOL/DME (1/1 v/v)	60/30/10	Carbon black	Na alginate	184	80, 0.5	90, 30	1.5	68a
127	Lithiation	7.0 M LiTFSI, DOL/DME (1/1 v/v)	60/30/10	Carbon black	Na alginate	346	220, 0.5	178, 100	1.47, 1.25	68b
130	Lithiation	7.0 M LiTFSI, DOL/DME (1/1 v/v)	60/30/10	Carbon black	Na alginate	190	190, 0.5	175, 100	1.5, 1.55	68a
131	Poly-condensation	1.0 M $TBAClO_4$, CH_3CN	5/85/10	VGCF	PVdF	158	95, 0.03	65, 10	0.65, 1.18	76
136	Hetero-arylation polymerization	1.0 M $LiPF_6$, EC/DEC/DMC (1/1/1 v/v/v)	30/60/10	Acetylene black	PVdF	104	33, 0.1	21, 10	2.2, 1.90	77
137	Hetero-arylation polymerization	1.0 M $LiPF_6$, EC/DEC/DMC (1/1/1 v/v/v)	30/60/10	Acetylene black	PVdF	72	56, 0.1	47, 10	2.2, 1.90	77

Table 1. continued

Materials	Method	Electrolyte	Electrode (active material/conductive additive/binder) [wt.%]	Additive	Binder	C_{th} [mAh·g^{-1}]	C_i [mAh·g^{-1}], rate	C_n [mAh·g^{-1}], Cycle number	Potential [V]	Ref.
138	Hetero-arylation polymerization	1.0 M $LiPF_6$, EC/DEC/DMC (1/1/1 v/v/v)	30/60/10	Acetylene black	PVdF	59	19, 0.1	17, 10	2.2, 1.90	77
	Poly-condensation	1.0 M $LiPF_6$, EMC/EC/DMC (1/1/1 v/v/v)	80/15/5	Acetylene black	PTFE	338	62, n.r.	10, 30	2.35–1.5	78
140	Poly-condensation	1.0 M LiTFSI, DOL/DME (1/1 v/v)	60/30/10	Printex XE2	PTFE	315	163, 0.2	156, 100	2.35	11b
141	Poly-condensation	1.0 M LiTFSI, DOL/DME (1/1 v/v)	60/30/10	Printex XE2	PTFE	406	202, 0.2	183, 100	2.47	11b
142	Poly-condensation	1.0 M $LiPF_6$, EC/DMC (1/1 v/v)	60/10/30	Carbon black	PVdF	n.r.	175, n.r.	153, 60	2.48	24a
143										

Table 1. continued

Materials	Method	Electrolyte	Electrode (active material/ conductive additive/binder) [wt.%]	Additive	Binder	C_{th} [mAh·g^{-1}]	C_i [mAh·g^{-1}], rate	C_n [mAh·g^{-1}], Cycle number	Potential [V]	Ref.
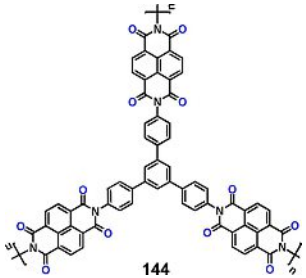 144	Poly-condensation	1.0 M $LiPF_6$, EMC/EC/ DMC (1/1/1 v/v/v)	80/15/5	Acetylene black	PTFE	292	103, n.r.	68.5, 30	2.35	78
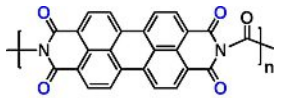 145	Poly-condensation	1.0 M $LiPF_6$, EC/DMC (1/1 v/v)	60/30/10	Acetylene black	PVdF	196.7	80, n.r.	130, 50	2.43	69a
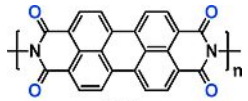 146	Poly-condensation	1.0 M $LiPF_6$, EC/DMC (1/1 v/v)	60/30/10	Acetylene black	PVdF	276	130, n.r.	120, 50	2.3	69a
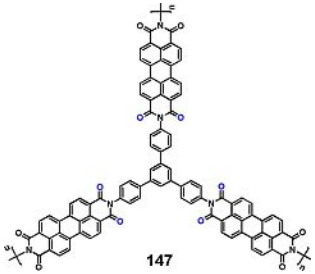 147	Poly-condensation	1.0 M $LiPF_6$, EMC/EC/ DMC (1/1/1 v/v/v)	80/15/5	Acetylene black	PTFE	109	78, n.r.	58, 65	2.5	78
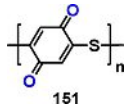 151	Phillips method + Oxidation	1.0 M LiTFSI, DOL/ DME (1/1 v/v)	60/30/10	Ketjen black	PTFE	388	232, n.r.	160, 1000	2.67	38
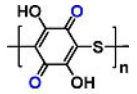 153	Phillips method	1.0 M LiTFSI, DOL/ DME (1/1 v/v)	60/30/10	Ketjen black	PTFE	315	214, n.r.	100, 20	2.3–1.75	80
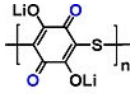 154	Phillips method + Lithiation	1.0 M LiTFSI, DOL/ DME (1/1 v/v)	60/30/10	Ketjen black	PTFE	295	268, n.r.	239, 1500	2.3–1.8	80

Table 1. continued

Materials	Method	Electrolyte	Electrode (active material/ conductive additive/binder) [wt.%]	Additive	Binder	C_{th} [mAh·g^{-1}]	C_i [mAh·g^{-1}], rate	C_n [mAh·g^{-1}], Cycle number	Potential [V]	Ref.
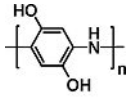	Oxidative polymerisation	1.0 M $LiPF_6$, EC/DEC (1/1 v/v)	60/30/10	Carbon black	PVdF	n.r.	80, 0.1	110, 50	2.8–2.0	81
157 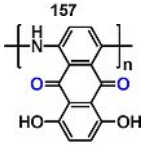	Oxidative polymerisation	1.0 M $LiPF_6$, EC/DEC (1/1 v/v)	50/40/10	Carbon black	PVdF	420	101, n.r.	129, 50	3.5–1.5	23b
159 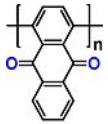	Ni-catalysed polycondensation	1.0 M LiTFSI, DOL/DME (1/1 v/v)	60/30/10	Carbon black	PTFE	260	260, 0.2	248, 1000	2.3	19b
161 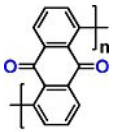	Ni-catalysed polycondensation	1.0 M LiTFSI, DOL/DME (1/1 v/v)	60/30/10	Carbon black	PTFE	260	230, 0.2 C	163, 100	2.3	19b
163 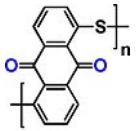	Phillips method	1.0 M LiTFSI, DOL/DME (1/1 v/v)	40/40/20	Acetylene black	PTFE	225	198, n.r.	178, 200	2.5–2.0	38
164 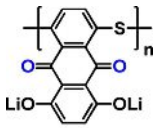	Phillips method	1.0 M LiTFSI, DOL/DME (2/1 v/v)	[50/50]/10	Carbon Super P	PTFE	380	300, 2	210, 1200	2.5	82
166 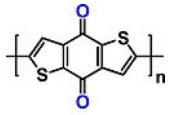 PBDTD, 169	Ni-catalysed polycondensation	1.0 M $LiClO_4$, DOL/DME (1/1 v/v)	60/30/10	19.1 wt.% CNTs, Carbon Super P	PTFE	n.r.	214, 5	175, 250	2.52	83
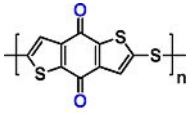 PBDTDS, 170	Phillips method	1.0 M $LiClO_4$, DOL/DME (1/1 v/v)	60/30/10	19.1 wt.% CNTs, Carbon Super P	PTFE	n.r.	200, 5	137, 250	2.56	83

materials with a structural variety are readily accessible via straightforward synthetic routes. Moreover, thanks to their chemical stability, processability and low cost, they could be promising candidates for high performance electrodes in LIBs technology. The discussed carbonyl-based π-conjugated compounds were classified depending on their chemical structure family from small organic molecules to polymeric framework with a detailed analysis of their synthesis and electrochemical performance as redox-active materials for LIBs. The structural versatility and the tunability of these organic compounds can take advantage of rich organic and polymer chemistries to develop more stable organic electrode materials with greater capacity, optimized output potential, improved stability, and ultimate non-solubility in solid-state batteries and thus the range of possible applications can be enlarged. The poor electrical conductivity of materials remains a primary impediment that continuously stimulates chemical modifications of the active materials. Theoretical effort could assist novel design strategies, for instance, for the introduction of specific units able to increase the electrical conductivity along the main chain backbone of the employed polymers.

Carbonyl-based molecules are widespread in nature; approaches to derive the active material from renewable resources through greener processes have appeared recently aiming to develop sustainable ESSs to meet the demands of a greener future.[4a,85] Depending on the type of the redox active materials, which can undergo chemically reversible oxidation or reduction, all-organic batteries can be built; thus, an organic n-type material would be applied as anode and a p-type material as cathode. Addressing the question of the electrode composition versus its cycling and reliability is key for progressing in this field. In Figure 3 we display, for available reported 0.2 C rate data for low molecular weight compounds (Table 1), for two different binders, the ratio of the initial discharge capacity to the theoretical capacity as a function of the active material loading. The architecture of the electrode greatly impacts the stability and the electron transfer rates. The electrode engineering has to proceed towards an increased loading of active compounds.

Efficient polymer electrolytes are largely missing, although some steps have been taken in this direction. The use of gel[86] or solid electrolyte (for example, polystyrene-*block*-poly(oligo (ethylene glycol) methacrylate) PS-*b*-POEGMA)[87] could suppress the major drawback of the solubility issue faced by organic redox-active compounds leading to safer all-organic batteries. The solubility concern can also be challenged via innovative composites of organic redox materials (with extended π-conjugated scaffolds or via heterogeneous co-doping with Si or P atoms) and hierarchically structured carbon materials able to accord electrochemical and solvation kinetics.[88] By using smart thermal treatments of these unique composites, with optimized thickness and composition, their stability could be reinforced.

Although the available organic electrode materials do not satisfy the market's requirements for grid-scale stationary energy storage systems or for the transportation sector in terms of high energy/power densities and cycling performance, a resurgence of interest has been induced by the ever-growing market for small, ultra-thin and mechanically flexible devices related to the Internet-of-Things deployment such as roll-up displays, medical devices, or active radio-frequency identification tags. For the best of our knowledge, all examples of π-conjugated carbonyl-based redox-active materials reported until now were tested in coin or Swagelok cells configurations with essentially no application of these materials on mechanically flexible substrates or smart integration in flexible electronics. Obviously, shaping, handling and tailoring of carbonyl-based electrodes is not straightforward. New techniques are required to facilitate their coherent integration into operational systems and miniaturized autonomous platforms could represent niche ESSs. Carbonyl-based π-conjugated redox-active materials are valuable candidates for the next generation of lightweight rechargeable batteries to fulfil the required features of softness, bendability and stretchability in printed electronic devices (Figure 4), yet more consistent reporting of both their rate performance and mechanical properties when integrated in electrodes is needed. The well-established printing techniques for electronic devices can be adapted to allow low-cost mass production.[89] Finally, we note that the good solubility of organic compounds in electrolytes, a drawback in organic batteries, could be a useful feature to be exploited for more environmentally friendly redox-flow battery systems compared to the current technology based on vanadium-based compounds in sulphuric acid.[89]

Acknowledgements

We are grateful to the Walloon Region for financial support in the frame of the "BATWAL" project – "Programme d'Excellence". This research was supported by the "Fonds européen de développement regional" and the Walloon region under the Operational Program "Wallonia-2020.EU" (project CLEARPOWER). The study partially benefited from the European Union through the Interreg V initiative France-Wallonie-Vlaanderen ("Fonds européen du développement regional" - projet LUMINOPTEX). The work received aid from the Belgian F.R.S. – FNRS in the frame of the research conventions n° T.1004.14 and n° T.0106.16. This research connects to the ARC project entitled "BATTAB" (research convention n° 14/19-057) sponsored by the Communauté Française de Belgique.

Conflict of Interest

The authors declare no conflict of interest.

Keywords: carbonyl compounds · electrochemistry · electrode materials · π-conjugated materials · organic lithium-ion batteries

[1] a) I. E. Agency, in *IEA, Vol. 2018*, **2018**; b) D. Larcher, J. M. Tarascon, *Nat. Chem.* **2014**, *7*, 19–29.
[2] a) F. Cheng, J. Liang, Z. Tao, J. Chen, *Adv. Mater.* **2011**, *23*, 1695–1715; b) in *UNFCCC*, United Nations Climate Change, **2018**.

[3] a) J. B. Goodenough, Y. Kim, *Chem. Mater.* **2010**, *22*, 587–603; b) J. Liu, J. Wang, C. Xu, H. Jiang, C. Li, L. Zhang, J. Lin, X. Shen Ze, *Adv. Sci.* **2017**, *5*, 1700322–1170040; c) N. S. Lewis, *Science* **2016**, *351*, 1920–1929.

[4] a) M. Miroshnikov, K. P. Divya, G. Babu, A. Meiyazhagan, L. M. Reddy Arava, P. M. Ajayan, G. John, *J. Mater. Chem. A* **2016**, *4*, 12370–12386; b) G. Crabtree, *Nature* **2015**, *526*, S92; c) A. G. Olabi, *Energy* **2017**, *136*, 1–6; d) X. Luo, J. Wang, M. Dooner, J. Clarke, *Appl. Energy* **2015**, *137*, 511–536; e) T. Kousksou, P. Bruel, A. Jamil, T. El Rhafiki, Y. Zeraouli, *Sol. Energy Mater. Sol. Cells* **2014**, *120*, 59–80; f) V. Etacheri, R. Marom, R. Elazari, G. Salitra, D. Aurbach, *Energy Environ. Sci.* **2011**, *4*, 3243–3262; g) L. Lu, X. Han, J. Li, J. Hua, M. Ouyang, *J. Power Sources* **2013**, *226*, 272–288.

[5] a) H. Chen, T. N. Cong, W. Yang, C. Tan, Y. Li, Y. Ding, *Prog. Nat. Sci.* **2009**, *19*, 291–312; b) M. Aneke, M. Wang, *Appl. Energy* **2016**, *179*, 350–377; c) S. Lee, G. Kwon, K. Ku, K. Yoon, S. K. Jung, H. D. Lim, K. Kang, *Adv. Mater.* **2018**, 1704682; d) M. Armand, J. M. Tarascon, *Nature* **2008**, *451*, 652–657; e) P. G. Bruce, S. A. Freunberger, L. J. Hardwick, J.-M. Tarascon, *Nat. Mater.* **2011**, *11*, 19–29; f) N. Nitta, F. Wu, J. T. Lee, G. Yushin, *Mater. Today* **2015**, *18*, 252–264; g) D. Deng, *Eng. Sci.* **2015**, *3*, 385–418; h) J. B. Goodenough, K.-S. Park, *J. Am. Chem. Soc.* **2013**, *135*, 1167–1176; i) R. Chen, R. Luo, Y. Huang, F. Wu, L. Li, *Adv. Sci.* **2016**, *3*, 1600051.

[6] a) G. E. Blomgren, *J. Electrochem. Soc.* **2017**, *164*, A5019-A5025; b) B. Scrosati, J. Hassoun, Y.-K. Sun, *Energy Environ. Sci.* **2011**, *4*, 3287–3295.

[7] a) A. Yoshino, *Angew. Chem. Int. Ed.* **2012**, *51*, 5798–5800; *Angew. Chem.* **2012**, *124*, 5898–5900; b) Y. Nishi, *Chem. Rec.* **2001**, *1*, 406–413.

[8] a) Y. Mekonnen, A. Sundararajan, A. I. Sarwat, *SoutheastCon 2016*, **2016**, 1–6; b) A. Manthiram, *ACS Cent. Sci.* **2017**, *3*, 1063–1069; c) A. Vlad, A. L. M. Reddy, A. Ajayan, N. Singh, J.-F. Gohy, S. Melinte, P. M. Ajayan, *Proc. Mont. Acad. Sci.* **2012**, *109*, 15168; d) G. Sandu, M. Coulombier, V. Kumar, H. G. Kassa, I. Avram, R. Ye, A. Stopin, D. Bonifazi, J.-F. Gohy, P. Leclère, X. Gonze, T. Pardoen, A. Vlad, S. Melinte, *Sci. Rep.* **2018**, *8*, 9794.

[9] a) H. Vikström, S. Davidsson, M. Höök, *Appl. Energy* **2013**, *110*, 252–266; b) T. P. Narins, *Extr. Ind. Soc.* **2017**, *4*, 321–328; c) J. Speirs, M. Contestabile, Y. Houari, R. Gross, *Renewable Sustainable Energy Rev.* **2014**, *35*, 183–193; d) J. Cabana, L. Monconduit, D. Larcher, M. R. Palacín, *Adv. Mater.* **2010**, *22*, E170-E192; e) O. Schmidt, A. Hawkes, A. Gambhir, I. Staffell, *Nat. Energy* **2017**, *2*, 17110; f) A. Stephan, B. Battke, M. D. Beuse, J. H. Clausdeinken, T. S. Schmidt, *Nat. Energy* **2016**, *1*, 16079; g) T. A. Faunce, J. Prest, D. Su, S. J. Hearne, F. Iacopi, *MRS Energy Sustainability* **2018**, *5*, E11.

[10] a) E. C. Evarts, *Nature* **2015**, *526*, S93; b) D. Di Lecce, R. Verrelli, J. Hassoun, *Green Chem.* **2017**, *19*, 3442–3467; c) A. Mauger, C. M. Julien, *Ionics* **2017**, *23*, 1933–1947.

[11] a) R. Cao, J. Qian, J.-G. Zhang, W. Xu, in *Rechargeable Batteries: Materials, Technologies and New Trends* (Eds.: Z. Zhang, S. S. Zhang), Springer International Publishing, Cham, **2015**, pp. 637–671; b) Z. Song, H. Zhan, Y. Zhou, *Angew. Chem.* **2010**, *122*, 8622–8626; *Angew. Chem. Int. Ed.* **2010**, *49*, 8444–8448; c) Z. Song, H. Zhan, Y. Zhou, *Angew. Chem. Int. Ed.* **2010**, *49*, 8444–8448; *Angew. Chem.* **2010**, *122*, 8622–8626.

[12] a) R. Schroot, M. Jager, U. S. Schubert, *Chem. Soc. Rev.* **2017**, *46*, 2754–2798; b) H. Shirakawa, E. J. Louis, A. G. MacDiarmid, C. K. Chiang, A. J. Heeger, *J. Chem. Soc. Chem. Commun.* **1977**, 578–580; c) D. MacInnes, M. A. Druy, P. J. Nigrey, D. P. Nairns, A. G. MacDiarmid, A. J. Heeger, *J. Chem. Soc. Chem. Commun.* **1981**, 317–319; d) L. Yang, W. Qiu, Q. Liu, *Solid State Ionics* **1996**, *86–88*, 819–824; e) M. Armand, S. Grugeon, H. Vezin, S. Laruelle, P. Ribière, P. Poizot, J. M. Tarascon, *Nat. Mater.* **2009**, *8*, 120–125; f) P. Novák, K. Müller, K. S. V. Santhanam, O. Haas, *Chem. Rev.* **1997**, *97*, 207–282; g) S. Miller Joel, *Adv. Mater.* **1993**, *5*, 671–676; h) Z. Song, H. Zhou, *Energy Environ. Sci.* **2013**, *6*, 2280–2301; i) Y. Zhang, J. Wang, S. N. Riduan, *J. Mater. Chem. A* **2016**, *4*, 14902–14914.

[13] a) P. Poizot, F. Dolhem, *Energy Environ. Sci.* **2011**, *4*, 2003–2019; b) H. Chen, M. Armand, G. Demailly, F. Dolhem, P. Poizot, J. M. Tarascon, *ChemSusChem* **2008**, *1*, 348–355.

[14] a) T. Janoschka, D. Hager Martin, S. Schubert Ulrich, *Adv. Mater.* **2012**, *24*, 6397–6409; b) S. Wang, L. Wang, K. Zhang, Z. Zhu, Z. Tao, J. Chen, *Nano Lett.* **2013**, *13*, 4404–4409; c) X. Wang, Q. Weng, Y. Yang, Y. Bando, D. Golberg, *Chem. Soc. Rev.* **2016**, *45*, 4042–4073; d) C. Liu, Z. G. Neale, G. Cao, *Mater. Today* **2016**, *19*, 109–123.

[15] D. L. Williams, J. J. Byrne, J. S. Driscoll, *J. Electrochem. Soc.* **1969**, *116*, 2–4.

[16] a) P. J. Nigrey, D. MacInnes, D. P. Nairns, A. G. MacDiarmid, A. J. Heeger, *J. Electrochem. Soc.* **1981**, *128*, 1651–1654; b) R. Balint, N. J. Cassidy, S. H. Cartmell, *Acta Biomater.* **2014**, *10*, 2341–2353; c) Z. A. Boeva, V. G. Sergeyev, *Polym. Sci. Ser. C* **2014**, *56*, 144–153; d) L. M. Zhu, W. Shi, R. R. Zhao, Y. L. Cao, X. P. Ai, A. W. Lei, H. X. Yang, *J. Electroanal. Chem.* **2013**, *688*, 118–122; e) L. Qie, L.-X. Yuan, W.-X. Zhang, W.-M. Chen, Y.-H. Huang, *J. Electrochem. Soc.* **2012**, *159*, 1624–1629; f) D. Aradilla, F. Estrany, F. Casellas, J. I. Iribarren, C. Alemán, *Org. Electron.* **2014**, *15*, 40–46; g) S. K. Simotwo, V. Kalra, *Curr. Opin. Chem. Eng.* **2016**, *13*, 150–160; h) H. Wang, J. Lin, Z. X. Shen, *J. Sci.: Adv. Mater. Devices* **2016**, *1*, 225–255; i) G. Sandu, B. Ernould, J. Rolland, N. Cheminet, J. Brassinne, P. R. Das, Y. Filinchuk, L. Cheng, L. Komsiyska, P. Dubois, S. Melinte, J.-F. Gohy, R. Lazzaroni, A. Vlad, *ACS Appl. Mater. Interfaces* **2017**, *9*, 34865–34874.

[17] Y. Liang, Z. Tao, J. Chen, *Adv. Energy Mater.* **2012**, *2*, 742–769.

[18] a) J. Kim, J. H. Kim, K. Ariga, *Joule* **2017**, *1*, 739–768; b) E. P. Tomlinson, M. E. Hay, B. W. Boudouris, *Macromolecules* **2014**, *47*, 6145–6158; c) K. Nakahara, K. Oyaizu, H. Nishide, *Chem. Lett.* **2011**, *40*, 222–227; d) K. Oyaizu, H. Nishide, *Adv. Mater.* **2009**, *21*, 2339–2344; e) K. Nakahara, S. Iwasa, M. Satoh, Y. Morioka, J. Iriyama, M. Suguro, E. Hasegawa, *Chem. Phys. Lett.* **2002**, *359*, 351–354; f) A. Vlad, N. Singh, J. Rolland, S. Melinte, P. M. Ajayan, J. F. Gohy, *Sci. Rep.* **2014**, *4*, 4315; g) B. Ernould, M. Devos, J.-P. Bourgeois, J. Rolland, A. Vlad, J.-F. Gohy, *J. Mater. Chem. A* **2015**, *3*, 8832–8839; h) G. Hauffman, A. Vlad, T. Janoschka, U. S. Schubert, J. F. Gohy, *J. Mater. Chem. A* **2015**, *3*, 19575–19581; i) A. Vlad, N. Singh, S. Melinte, J. F. Gohy, P. M. Ajayan, *Sci. Rep.* **2016**, *6*, 22194; j) B. Ernould, O. Bertrand, A. Minoia, R. Lazzaroni, A. Vlad, J.-F. Gohy, *RSC Adv.* **2017**, *7*, 17301–17310; k) A. Aqil, A. Vlad, M.-L. Piedboeuf, M. Aqil, N. Job, S. Melinte, C. Detrembleur, C. Jérôme, *Chem. Commun.* **2015**, *51*, 9301–9304.

[19] a) B. Häupler, A. Wild, S. Schubert Ulrich, *Adv. Energy Mater.* **2015**, *5*, 1402034; b) Z. Song, Y. Qian, L. Gordin Mikhail, D. Tang, T. Xu, M. Otani, H. Zhan, H. Zhou, D. Wang, *Angew. Chem. Int. Ed.* **2015**, *54*, 13947–13951; *Angew. Chem.* **2015**, *127*, 14153–14157; c) M. Tang, H. Li, E. Wang, C. Wang, *Chin. Chem. Lett.* **2018**, *29*, 232–244.

[20] a) S. Muench, A. Wild, C. Friebe, B. Häupler, T. Janoschka, U. S. Schubert, *Chem. Rev.* **2016**, *116*, 9438–9484; b) T. B. Schon, B. T. McAllister, P.-F. Li, D. S. Seferos, *Chem. Soc. Rev.* **2016**, *45*, 6345–6404; c) J. Xie, Q. Zhang, *J. Mater. Chem. A* **2016**, *4*, 7091–7106.

[21] a) Y. Xu, M. Zhou, Y. Lei, *Mater. Today* **2018**, *21*, 60–78; b) H. Alt, H. Binder, A. Köhling, G. Sandstede, *Electrochim. Acta* **1972**, *17*, 873–887.

[22] X. Han, C. Chang, L. Yuan, T. Sun, J. Sun, *Adv. Mater.* **2007**, *19*, 1616–1621.

[23] a) Y. Wu, R. Zeng, J. Nan, D. Shu, Y. Qiu, S. L. Chou, *Adv. Energy Mater.* **2017**, *7*, 1700278; b) L. Zhao, W. Wang, A. Wang, K. Yuan, S. Chen, Y. Yang, *J. Power Sources* **2013**, *233*, 23–27.

[24] a) C. Chen, X. Zhao, H.-B. Li, F. Gan, J. Zhang, J. Dong, Q. Zhang, *Electrochim. Acta* **2017**, *229*, 387–395; b) J. Lee, A. J. Kalin, T. Yuan, M. Al-Hashimi, L. Fang, *Chem. Sci.* **2017**, *8*, 2503–2521.

[25] Q. Zhao, C. Guo, Y. Lu, L. Liu, J. Liang, J. Chen, *Ind. Eng. Chem. Res.* **2016**, *55*, 5795–5804.

[26] S. Renault, J. Geng, F. Dolhem, P. Poizot, *Chem. Commun.* **2011**, *47*, 2414–2416.

[27] a) Y. Liang, P. Zhang, J. Chen, *Chem. Sci.* **2013**, *4*, 1330–1337; b) G. S. Vadehra, R. P. Maloney, M. A. Garcia-Garibay, B. Dunn, *Chem. Mater.* **2014**, *26*, 7151–7157; c) D. J. Kim, S. H. Je, S. Sampath, J. W. Choi, A. Coskun, *RSC Adv.* **2012**, *2*, 7968–7970.

[28] a) M. E. Bhosale, K. Krishnamoorthy, *Chem. Mater.* **2015**, *27*, 2121–2126; b) X. Zhu, X. Liu, W. Deng, L. Xiao, H. Yang, Y. Cao, *Mater. Lett.* **2016**, *175*, 191–194.

[29] C. Huang, S. Barlow, S. R. Marder, *J. Org. Chem.* **2011**, *76*, 2386–2407.

[30] C. Sotiriou-Leventis, Z. Mao, *J. Heterocycl. Chem.* **2009**, *37*, 1665–1667.

[31] P. R. Ashton, S. E. Boyd, A. Brindle, S. J. Langford, S. Menzer, L. Pe′rez-García, J. A. Preece, i. M. Raymo, N. Spencer, J. Fraser Stoddart, A. J. P. White, D. J. Williams, *New J. Chem.* **1999**, *23*, 587–602.

[32] A. E. Lakraychi, K. Fahsi, L. Aymard, P. Poizot, F. Dolhem, J. P. Bonnet, *Electrochem. Commun.* **2017**, *76*, 47–50.

[33] M. Lv, F. Zhang, Y. Wu, M. Chen, C. Yao, J. Nan, D. Shu, R. Zeng, H. Zeng, S.-L. Chou, *Sci. Rep.* **2016**, *6*, 23515.

[34] Y.-L. Wu, N. E. Horwitz, K.-S. Chen, D. A. Gomez-Gualdron, N. S. Luu, L. Ma, T. C. Wang, M. C. Hersam, J. T. Hupp, O. K. Farha, R. Q. Snurr, M. R. Wasielewski, *Nat. Chem.* **2016**, *9*, 466–472.

[35] T. Ohzuku, H. Wakamatsu, Z. Takehara, S. Yoshizawa, *Electrochim. Acta* **1979**, *24*, 723–726.

[36] a) X. Han, G. Qing, J. Sun, T. Sun, *Angew. Chem. Int. Ed.* **2012**, *51*, 5147–5151; *Angew. Chem.* **2012**, *124*, 5237–5241; b) X. Han, G. Qing, J. Sun, T. Sun, *Angew. Chem.* **2012**, *124*, 5237–5241; *Angew. Chem. Int. Ed.* **2012**, *51*, 5147–5151.

[37] J. Xie, W. Chen, Z. Wang, K. C. W. Jie, M. Liu, Q. Zhang, *Chem. Asian J.* **2017**, *12*, 868–876.

[38] Z. Song, Y. Qian, T. Zhang, M. Otani, H. Zhou, *Adv. Sci.* **2015**, *2*, 1500124.

[39] a) Q. Zhao, Y. Lu, J. Chen, *Adv. Energy Mater.* **2016**, *7*, 1601792; b) Q. Zhao, Z. Zhu, J. Chen, *Adv. Mater.* **2017**, *29*, 1607007.
[40] L. Chen, S. Liu, L. Zhao, Y. Zhao, *Electrochim. Acta* **2017**, *258*, 677–683.
[41] C. Wang, Y. Xu, Y. Fang, M. Zhou, L. Liang, S. Singh, H. Zhao, A. Schober, Y. Lei, *J. Am. Chem. Soc.* **2015**, *137*, 3124–3130.
[42] T. Yokoji, H. Matsubara, M. Satoh, *J. Mater. Chem. A* **2014**, *2*, 19347–19354.
[43] H. Matsubara, T. Maegawa, Y. Kita, T. Yokoji, A. Nomoto, *Org. Biomol. Chem.* **2014**, *12*, 5442–5447.
[44] Z. Luo, L. Liu, Q. Zhao, F. Li, J. Chen, *Angew. Chem. Int. Ed.* **2017**, *56*, 12561–12565; *Angew. Chem.* **2017**, *129*, 12735–12739.
[45] K. C. Kim, T. Liu, S. W. Lee, S. S. Jang, *J. Am. Chem. Soc.* **2016**, *138*, 2374–2382.
[46] T. Boschi, R. Pappa, G. Pistoia, M. Tocci, *J. Electroanal. Chem. Interfacial Electrochem.* **1984**, *176*, 235–242.
[47] M. Pasquali, G. Pistoia, T. Boschi, P. Tagliatesta, *Solid State Ionics* **1987**, *23*, 261–266.
[48] Q. Zou, W. Wang, A. Wang, Z. Yu, K. Yuan, *Mater. Lett.* **2014**, *117*, 290–293.
[49] H. Chen, M. Armand, M. Courty, M. Jiang, C. P. Grey, F. Dolhem, J.-M. Tarascon, P. Poizot, *J. Am. Chem. Soc.* **2009**, *131*, 8984–8988.
[50] A.-L. Barrès, J. Geng, G. Bonnard, S. Renault, S. Gottis, O. Mentré, C. Frayret, F. Dolhem, P. Poizot, *Chem. Eur. J.* **2012**, *18*, 8800–8812.
[51] W. Gorecki, M. Jeannin, E. Belorizky, C. Roux, M. Armand, *J. Phys. Condens. Matter* **1995**, *7*, 6823.
[52] M. Nagao, Y. Imade, H. Narisawa, T. Kobayashi, R. Watanabe, T. Yokoi, T. Tatsumi, R. Kanno, *J. Power Sources* **2013**, *222*, 237–242.
[53] M. Lécuyer, J. Gaubicher, A.-L. Barrès, F. Dolhem, M. Deschamps, D. Guyomard, P. Poizot, *Electrochem. Commun.* **2015**, *55*, 22–25.
[54] R.-h. Zeng, X.-p. Li, Y.-c. Qiu, W.-s. Li, J. Yi, D.-s. Lu, C.-l. Tan, M.-q. Xu, *Electrochem. Commun.* **2010**, *12*, 1253–1256.
[55] A. Shimizu, H. Kuramoto, Y. Tsujii, T. Nokami, Y. Inatomi, N. Hojo, H. Suzuki, J.-i. Yoshida, *J. Power Sources* **2014**, *260*, 211–217.
[56] J. Lee, H. Kim, M. J. Park, *Chem. Mater.* **2016**, *28*, 2408–2416.
[57] W. Wan, H. Lee, X. Yu, C. Wang, K.-W. Nam, X.-Q. Yang, H. Zhou, *RSC Adv.* **2014**, *4*, 19878–19882.
[58] H. H. Lee, Y. Park, K.-H. Shin, K. T. Lee, S. Y. Hong, *ACS Appl. Mater. Interfaces* **2014**, *6*, 19118–19126.
[59] A. E. Lakraychi, F. Dolhem, F. Djedaïni-Pilard, M. Becuwe, *Electrochem. Commun.* **2018**, *93*, 71–75.
[60] A. E. Lakraychi, F. Dolhem, F. Djedaïni-Pilard, A. Thiam, C. Frayret, M. Becuwe, *J. Power Sources* **2017**, *359*, 198–204.
[61] S. Renault, V. A. Oltean, C. M. Araujo, A. Grigoriev, K. Edström, D. Brandell, *Chem. Mater.* **2016**, *28*, 1920–1926.
[62] K. Park, J.-M. You, S. Jeon, S. Lee, *Eur. J. Org. Chem.* **2013**, *2013*, 1973–1978.
[63] a) J. Wu, X. Rui, C. Wang, W.-B. Pei, R. Lau, Q. Yan, Q. Zhang, *Adv. Energy Mater.* **2015**, *5*, 1402189; b) H. Yang, S. Liu, L. Cao, S. Jiang, H. Hou, *J. Mater. Chem. A* **2018**, *6*, 21216–21224.
[64] W. Walker, S. Grugeon, H. Vezin, S. Laruelle, M. Armand, F. Wudl, J.-M. Tarascon, *J. Mater. Chem.* **2011**, *21*, 1615–1620.
[65] L. Fédèle, F. Sauvage, J. Bois, J.-M. Tarascon, M. Bécuwe, *J. Electrochem. Soc.* **2014**, *161*, A46-A52.
[66] R. R. Zhao, Y. L. Cao, X. P. Ai, H. X. Yang, *J. Electroanal. Chem.* **2013**, *688*, 93–97.
[67] L. Fédèle, F. Sauvage, M. Bécuwe, *J. Mater. Chem. A* **2014**, *2*, 18225–18228.
[68] a) C. Luo, O. Borodin, X. Ji, S. Hou, K. J. Gaskell, X. Fan, J. Chen, T. Deng, R. Wang, J. Jiang, C. Wang, *Proc. Mont. Acad. Sci.* **2018**, *115*, 2004; b) C. Luo, X. Ji, S. Hou, N. Eidson, X. Fan, Y. Liang, T. Deng, J. Jiang, C. Wang, *Adv. Mater.* **2018**, *30*, 1706498.
[69] a) P. Sharma, D. Damien, K. Nagarajan, M. M. Shaijumon, M. Hariharan, *J. Phys. Chem. Lett.* **2013**, *4*, 3192–3197; b) H. g. Wang, S. Yuan, D. l. Ma, X. l. Huang, F. l. Meng, X. b. Zhang, *Adv. Energy Mater.* **2013**, *4*, 1301651.
[70] a) L. Nyholm, G. Nyström, A. Mihranyan, M. Strømme, *Adv. Mater.* **2011**, *23*, 3751–3769; b) C. Wang, W. Zheng, Z. Yue, C. O. Too, G. G. Wallace, *Adv. Mater.* **2011**, *23*, 3580–3584; c) L. Hu, M. Pasta, F. La Mantia, L. Cui, S. Jeong, H. D. Deshazer, J. W. Choi, S. M. Han, Y. Cui, *Nano Lett.* **2010**, *10*, 708–714; d) C. Yu, C. Masarapu, J. Rong, B. Wei, H. Jiang, *Adv. Mater.* **2009**, *21*, 4793–4797; e) B. Yue, C. Wang, X. Ding, G. G. Wallace, *Electrochim. Acta* **2012**, *68*, 18–24; f) J. Sun, Y. Huang, C. Fu, Z. Wang, Y. Huang, M. Zhu, C. Zhi, H. Hu, *Nano Energy* **2016**, *27*, 230–237; g) H.-P. Cong, X.-C. Ren, P. Wang, S.-H. Yu, *Energy Environ. Sci.* **2013**, *6*, 1185–1191; h) K. Sakaushi, G. Nickerl, F. M. Wisser, D. Nishio-Hamane, E. Hosono, H. Zhou, S. Kaskel, J. Eckert, *Angew. Chem. Int. Ed.* **2012**, *51*, 7850–7854; *Angew. Chem.* **2012**, *124*, 7972–7976; i) T. Nokami, T. Matsuo, Y. Inatomi, N. Hojo, T. Tsukagoshi, H. Yoshizawa, A. Shimizu, H. Kuramoto, K. Komae, H. Tsuyama, J.-i. Yoshida, *J. Am. Chem. Soc.* **2012**, *134*, 19694–19700; j) G. Nyström, A. Razaq, M. Strømme, L. Nyholm, A. Mihranyan, *Nano Lett.* **2009**, *9*, 3635–3639.
[71] a) H. Münstedt, G. Köhler, H. Möhwald, D. Naegele, R. Bitthin, G. Ely, E. Meissner, *Synth. Met.* **1987**, *18*, 259–264; b) T. Matsunaga, H. Daifuku, T. Nakajima, T. Kawagoe, *Polym. Adv. Technol.* **1990**, *1*, 33–39.
[72] Y. Meng, H. Wu, Y. Zhang, Z. Wei, *J. Mater. Chem. A* **2014**, *2*, 10842–10846.
[73] a) K. Liu, J. Zheng, G. Zhong, Y. Yang, *J. Mater. Chem.* **2011**, *21*, 4125–4131; b) I. Gomez, O. Leonet, J. Alberto Blazquez, H.-J. Grande, D. Mecerreyes, *ACS Macro Lett.* **2018**, *7*, 419–424.
[74] a) J. Drobny, in *Specialty Thermoplastics* (Ed.: J. Drobny), Springer Berlin Heidelberg, Berlin, Heidelberg, **2015**, pp. 70–73; b) G. M. Bower, L. W. Frost, *J. Polym. Sci. Part A* **1963**, *1*, 3135–3150; c) M. Al Kobaisi, S. V. Bhosale, K. Latham, A. M. Raynor, S. V. Bhosale, *Chem. Rev.* **2016**, *116*, 11685–11796.
[75] a) O. Ostroverkhova, *Chem. Rev.* **2016**, *116*, 13279–13412; b) J. Kuwabara, *Polym. J.* **2018**, *50*, 1099–1106.
[76] K. Oyaizu, A. Hatemata, W. Choi, H. Nishide, *J. Mater. Chem.* **2010**, *20*, 5404–5410.
[77] N. Zindy, J. T. Blaskovits, C. Beaumont, J. Michaud-Valcourt, H. Saneifar, P. A. Johnson, D. Bélanger, M. Leclerc, *Chem. Mater.* **2018**, *30*, 6821–6830.
[78] D. Tian, H.-Z. Zhang, D.-S. Zhang, Z. Chang, J. Han, X.-P. Gao, X.-H. Bu, *RSC Adv.* **2014**, *4*, 7506–7510.
[79] a) G. Manecke, W. Storck, *Angew. Chem. Int. Ed. Engl.* **1962**, *1*, 659–660; b) G. Manecke, W. Storck, *J. Polym. Sci. Part C* **1963**, *4*, 1457–1466.
[80] Z. Song, Y. Qian, X. Liu, T. Zhang, Y. Zhu, H. Yu, M. Otani, H. Zhou, *Energy Environ. Sci.* **2014**, *7*, 4077–4086.
[81] A. Vlad, K. Arnould, B. Ernould, L. Sieuw, J. Rolland, J.-F. Gohy, *J. Mater. Chem. A* **2015**, *3*, 11189–11193.
[82] A. Petronico, L. Bassett Kimberly, G. Nicolau Bruno, A. Gewirth Andrew, G. Nuzzo Ralph, *Adv. Energy Mater.* **2017**, *8*, 1700960.
[83] Y. Jing, Y. Liang, S. Gheytani, Y. Yao, *Nano Energy* **2017**, *37*, 46–52.
[84] B. Häupler, T. Hagemann, C. Friebe, A. Wild, U. S. Schubert, *ACS Appl. Mater. Interfaces* **2015**, *7*, 3473–3479.
[85] a) P. Ravichandiran, R. Kannan, A. Ramasubbu, S. Muthusubramanian, V. K. Samuel, *J. Saudi Chem. Soc.* **2016**, *20*, S93-S99; b) A. L. M. Reddy, S. Nagarajan, P. Chumyim, S. R. Gowda, P. Pradhan, S. R. Jadhav, M. Dubey, G. John, P. M. Ajayan, *Sci. Rep.* **2012**, *2*, 960–960.
[86] W. Li, Y. Pang, J. Liu, G. Liu, Y. Wang, Y. Xia, *RSC Adv.* **2017**, *7*, 23494–23501.
[87] J. Rolland, J. Brassinne, J. P. Bourgeois, E. Poggi, A. Vlad, J. F. Gohy, *J. Mater. Chem. A* **2014**, *2*, 11839–11846.
[88] J. Kim, R. Kumar, A. J. Bandodkar, J. Wang, *Adv. Electron. Mater.* **2017**, *3*, 1600260.
[89] C. Ding, H. Zhang, X. Li, T. Liu, F. Xing, *J. Phys. Chem. Lett.* **2013**, *4*, 1281–1294.

Manuscript received: December 15, 2018
Revised manuscript received: March 3, 2019